A review of parametrization schemes for land surface processes

By **Pedro Viterbo**

ECMWF, Shinfield Park, Reading, England

Table of contents

1. INTRODUCTION

The parametrization of land surface processes (LSP) in numerical weather prediction (NWP) or climate general

© ECMWF, 2002

circulation models (GCMs) is important for a number of reasons. First of all, the sensible and latent heat fluxes at the surface are the lower boundary conditions for the enthalpy and moisture equations in the atmosphere. The land surface schemes are also largely responsible for the quality of model produced near surface weather parameters, such as screen level temperature and dew point, and low level cloudiness. Furthermore, the surface conditions need to be such as to provide the adequate feedback mechanisms for the other physical processes in the atmosphere: low level cloudiness influences the surface radiative balance, sensible heat and latent heat fluxes influence the boundary layer exchanges and the intensity of the moist convective processes. Finally, the correct partitioning between sensible and latent heat fluxes determines the soil wetness, which acts as one of the forcings of low frequency atmospheric variability (Delworth and Manabe, 1988, 1989, Milly and Dunne, 1994). The soil layer acts - through its water content - as an integrator or low pass filter of the time series of rainfall. Understanding the soil wetness variability in the seasonal scale (e.g., extended drought periods), may lead to a better knowledge of low frequency atmospheric variability. Time series of soil moisture anomalies are primarily controlled by potential evaporation and the ratio of potential evaporation over precipitation (Milly, 1994).

The role played by continental and oceanic surfaces on the global heat budget of the atmosphere is illustrated by Fig. 1 . The mean atmospheric energy budget is shown in Fig. 1 (a) for all ECMWF forecasts verifying in August 1993; the *x*-axis specifies forecast days, the picture shows results from day 1 to day 10 in the forecast. For the whole atmosphere, the net radiative forcing is negative (the sign is reversed in the picture), implying a cooling of around 110 W m^{-2}, balanced by warming at the surface (sensible heat flux), and latent heat release corresponding to moist processes in the atmosphere. The surface sensible heat flux provides around 20% of the energy to balance the net radiative cooling. The moist processes (separated in the picture into convective processes and large-scale condensation) show a different level of activity at the beginning of the forecast range, because of initial imbalances in the thermal and humidity atmospheric fields (Arpe, 1991): in contrast, the sensible heat flux is almost constant during the forecast. Figs. 1 (b) and (c) show the surface energy budget for the same period, for all land points and for all sea points, respectively. Net solar radiation is the energy input to the surface, balanced by the sum of thermal radiation, latent and sensible heat fluxes, labelled total output in the panels (b) and (c). While the radiative fluxes are of the same order for land and sea, the partitioning of the available energy at the surface between latent and sensible heat flux is markedly different. The figures indicate a global value for the Bowen ratio (ratio of sensible heat flux over latent heat flux) of order 1 over the continents and 0.1 for the oceans, suggesting different physical mechanisms controlling the exchanges at the surface: i) the oceans have a larger thermal inertia, slower variations of the surface temperature, imbalances are allowed on a longer timescale; ii) the land masses have a faster responsive surface, the net heat flux at the surface (sum of the radiative fluxes, latent and sensible heat flux) is generally small. All the above balances are only exact (no residuals) at a global/annual timescale; at any particular period, and over a particular area, no exact balance is achieved, implying heat transport by the atmospheric circulation. The latent heat flux over land decreases 20% from day 1 to day 10 in the forecast, suggesting a drying of the surface throughout the forecast range, possibly due to either too much radiative solar energy at the surface or too much evaporation in the presence of correct solar fluxes.

© ECMWF, 2002

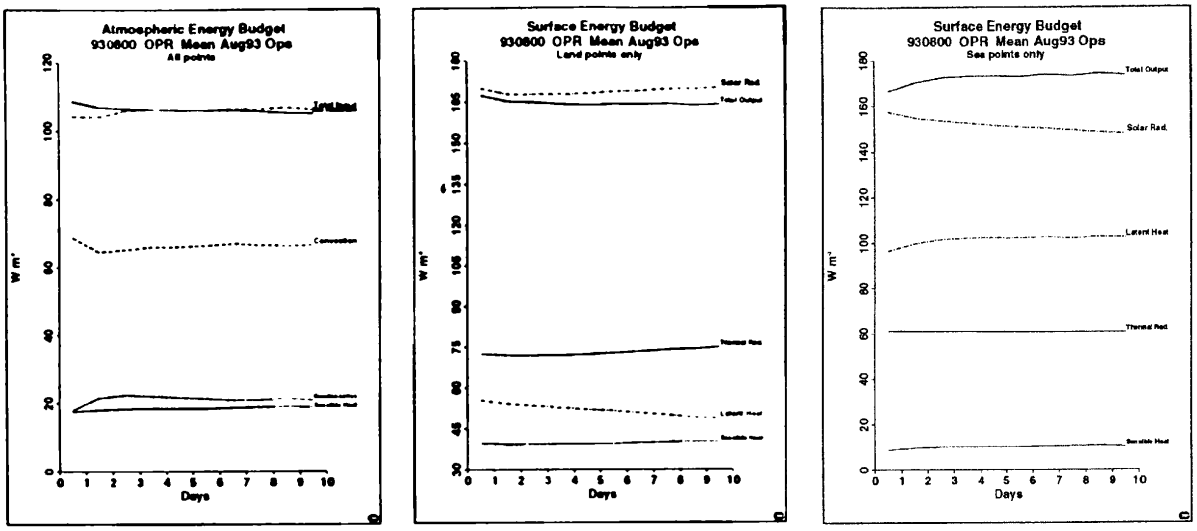

Figure 1. Mean atmospheric and surface energy budget for August 1993 ECMWF forecasts: (a) Atmospheric energy budget; (b) Surface energy budget for all land points; (c) As (b), but for all sea points.

Processes at the soil-vegetation-atmosphere interface, and their impact on GCMs are reviewed in Mintz (1984) and Garratt (1993). First studies on the role of soil water (Namias, 1958) led to the development of the so-called "bucket model" for evaporation and computation of surface runoff (Manabe, 1969). With the work of Deardorff (1978), the attention has somehow been switched from the role of soil water as a *slow* variable in the climatic system, to the contribution of the vegetation to the latent heat flux (evapotranspiration). Many of the schemes used today in GCMs (e.g. Dickinson *et al*., 1986; Sellers *et al*., 1986; Abramopoulos *et al*. , 1988; Noilhan and Planton, 1989) mimic the effect of plant physiology in using the amount of photosynthetic active solar radiation to regulate the opening and closing of leaf stomata, thus controlling the flow of water from the soil into the atmosphere and defining the transpiration rate. The concept of stomatal conductance as a product of different stress functions (Jarvis, 1976) is central to all the above models. On the other hand, many GCMs incorporate an interception reservoir, collecting rain and re-evaporating at the potential rate (Rutter *et al*., 1972).

The key issues in land surface parameterization are: i) the role of vegetation in controlling evapotranspiration and rainfall interception; ii) an adequate description of heat and water transfer in the soil; and iii) for high latitudes and over mountains a correct description of energy/water exchanges for the cryosphere. The direct influence of the land surface on timescales ranging from the diurnal cycle to the seasonal cycle is illustrated by the dual role of evaporation. Evaporation controls the amount of water kept in the soil during Spring, allowing its release during the Summer: in a climate model, systematic over-evaporation during the Spring means dry, warm Summer bias in the lower troposphere. However, for any particular Summer day, a wet surface will tend to evaporate more than a dry surface, and, for that reason, it will in general be cooler (see Section 2on combination equations): for that reason, an over-evaporation for a typical Summer day, generally means a cold, wet bias for the boundary layer. The role of land-surface parameterization in NWP models reflects these two apparently conflicting roles.

Recent reviews of methods for representing LSP in NWP and climate models include Garratt (1993), Bougeault (1991), Blondin (1991), Rowntree (1991), Avissar and Verstraete (1990), Laval (1988), Verstraete and Dickinson (1986). To the above, more general papers, one should add at least Dickinson *et al*. (1991), and Sellers (1992), for the role of the biosphere in controlling the evapotranspiration, Dickinson (1992), Stricker *et al*. (1993), and Shuttleworth (1993a), describing the role of the surface in relation to the climate system, and Dooge (1992a, 1992b),

© ECMWF, 2002

for an hydrologist perspective on the subject. In this review, no attempt will be made to give comprehensive descriptions of land surface parameterization schemes: the reader has a large choice of review papers in the literature. Instead, we will focus on a few issues that we consider relevant: the choice reflects work at ECMWF in recent years, in boundary layer aspects (Betts *et al*., 1993), and in the surface (Beljaars and Viterbo, 1994; Beljaars *et al*., 1995; Betts *et al*., 1995; Viterbo and Beljaars, 1995).

Section 2 presents some general remarks on the role of the surface, while in Section 3 the basic concepts of the soil energy and water budget are introduced: the role of vegetation versus bare ground on defining the evapotranspiration rate is described, the concepts of interception and surface runoff as perceived by large scale atmospheric models are presented, and the Penman–Monteith equation is derived as an example of an useful interpretative tool combining the heat and water budget in the soil. Section 4 presents three examples of parametrization schemes, with different complexity level. Section 5 discusses ways of representing subgrid scale heterogeneity, and methods for defining initial conditions for the surface variables. Brief remarks on validation and intercomparison are made on Section 6, while Section 7 deals with processes affecting the cryosphere. The concluding section emphasizes areas of uncertainty, and current needs for data. Throughout the paper the emphasis will be on simplicity and correct physical representation of the processes: In NWP the sensitivity to initial conditions prohibits the use of too complex LSP models, with a large number of surface parameters, while for climate modelling, the complexity of the more advanced LSP (e.g. SSiB, Xue *et al*., 1991) can be an advantage to handle correctly the atmospheric/surface interactions.

2. GENERAL REMARKS

Fig. 2 shows the size of the moisture reservoirs of the terrestrial atmosphere and the marine atmosphere, the exchanges of moisture between them, and between the atmosphere and the surface below. Surface evaporation over sea is more than 6 times as large as the corresponding value over land. The sea surface evaporates at the potential rate, while over land there are additional mechanisms that reduce the evapotranspiration rate: dryness of the soil or, over vegetated areas, physiological mechanisms that can reduce or shut transpiration from the plant leaves and trunks making the water from the root zone effectively unavailable for the atmosphere above. Precipitation over land is about a quarter of that over sea. Note that precipitation exceeds evaporation over land, while over sea the reverse is true. In order to have a closed budget for the terrestrial atmosphere, advection of moisture across a vertical wall projecting over the continent boundaries has to match the difference precipitation minus evaporation. Advection is roughly half of the water evaporated over land, suggesting an annual recirculation ratio (ratio of the rainfall coming from local evaporation over total rainfall rate) of 67% (71/107). To close the hydrological cycle, the advection has to be matched by the river runoff: the globally averaged influx of fresh water into the ocean, is estimated in this way as 36×10^{15} kg yr^{-1}. For continental areas, annual runoff, evaporation and precipitation are approximately in the ratio 1:2:3. The rainfall rate and the size of the terrestrial atmosphere reservoir can be combined to give a timescale 4.5/107=0.042 years=15 days: the terrestrial atmosphere reservoir would be emptied by rainfall in 15 days. In a similar way the reservoir would be replenished by surface evapotranspiration in 23 days (4.5/71 years). The timescales associated to marine rainfall are only 7.5 days, and the corresponding value for evaporation is 6.8 days. This suggests: i) a ore vigorous hydrologic cycle over the ocean; ii) a land surface control over large timescales (weeks to months), through the evapotranspiration flux of water at the surface. The implication of the above on the extended predictability of the atmosphere due to the exchanges of water with the land surface has been discussed in many papers see e.g., Namias, 1958, Mintz, 1984, Dümenil and Bengtsson, 1993, Dirmeyer and Shukla, 1993), and were already mentioned in Section 1.

© ECMWF, 2002

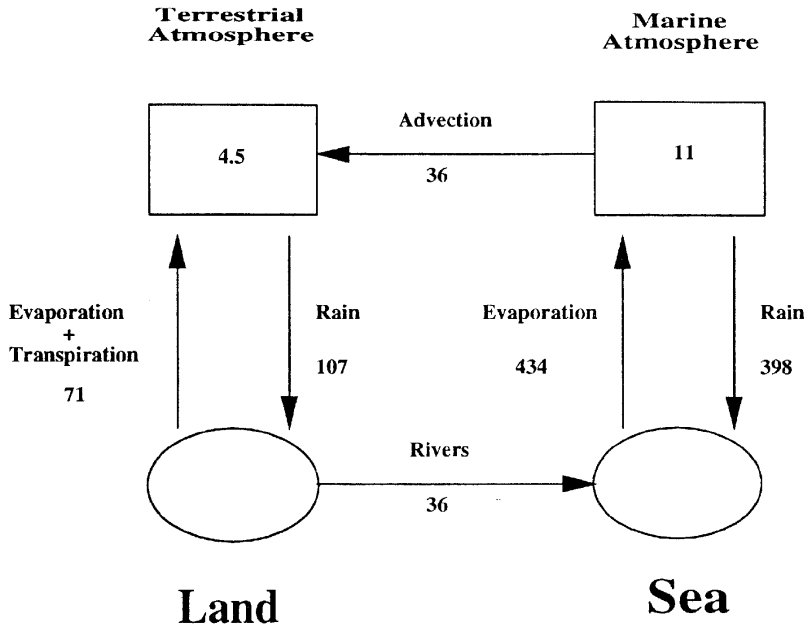

Figure 2. The global water cycle (from Chahine 1992). Units of water in the reservoirs: 10^{15} kg; units of water fluxes: 10^{15} kg yr^{-1}.

Before proceeding any further, in the interest of clarity we will now discuss a few conceptual notions of evaporation and define some basic quantities. Potential evaporation (PE) is the *amount of water evaporated per unit area, per unit time from an idealized extensive free water surface under existing atmospheric conditions* (Shuttleworth, 1993b). Several problems exist with this concept (see Brutsaert, 1982 for a thorough discussion). First, potential evaporation is often estimated based on measured near surface atmospheric conditions, which correspond to the idealized situation described above only shortly after an episode of precipitation or dew deposition. The amount of water in the soil conditions the actual evaporation, which, for a given incident radiation, determines the actual values of surface air temperature and humidity. If the soil was *an idealized extensive free water surface* the measured values of air temperature and humidity would change from its actual values. This sort of ambiguity has been the source of confusion in the literature about how to compute PE in atmospheric models: Pan (1990) present a method for its estimation, by use of a modified near surface air temperature, and Milly (1992) shows that this estimate matches early PE definitions of Manabe (1969) and Budyko (1974).

The other problem of potential evaporation is its failure to recognize the role of the surface cover. As detailed in following sections, the surface water vapour flux from a patchy natural covered surface is the sum of different contributions: the lakes and rivers, the bare ground, the wet fraction of the canopy, and plant transpiration from stems, leaves and trunks. When compared to the other contributions, plant transpiration has an additional resistance to the water vapour flux, dependent on physiological conditions, soil state and environmental factors. The maximum possible value of transpiration, so-called *unstressed evaporation* or *potential evapotranspiration* (Penman, 1948) corresponds to a minimum (non-zero) value of this resistance. If, in order to obtain the idealized *free water surface* defining PE, we do not change the roughness length, unstressed evaporation is always smaller than potential evaporation. Following common use in the literature, we will distinguish between *evaporation at the potential rate* (when the canopy is wet) and unstressed evaporation. Notwithstanding the problems referred above for its definition, PE is still a very useful concept as an upper "energy-limit" value of evaporation, for a given incident energy at the surface (Milly, 1993).

© ECMWF, 2002

A synthetic illustration of the interactions between the land surface and the atmosphere is presented in Fig. 3 , adapted from Dooge (1992a). The diagram illustrates the behaviour of the soil and the atmosphere within a complete idealized cycle composed of a wet period followed by a dry period. Let us start just after a long episode of rainfall, point A in the picture. The soil water is available in abundance in the root layer (for a precise definition of the concept of field capacity referred in the picture see Section 3.3 (b)), and its evolution (drying) is going to be determined by evaporation. While the soil has plenty of water, the rate of evaporation is controlled by the atmospheric moisture content in the near-surface: the regime is *controlled by the atmosphere* and the evaporation is at the potential rate. Below a certain level of soil moisture (point B in the picture), physiological mechanisms will limit the supply of water from the root layer into the atmosphere, and evaporation will drop below its maximum value (potential rate). The regime is under a *soil (vegetation) control*. When precipitation starts (point C), it will meet a soil dry enough during the initial stages, so that infiltration (the amount of water that falls as precipitation and is effectively collected by the soil for future use) will equal precipitation. The evolution of water in the soil is once more *atmospheric controlled*, via the rate of precipitation. Beyond a certain value of soil water (point D), the soil does not have the ability to infiltrate all precipitation, some of it goes into runoff. This last phase is again *soil controlled*: the state of the soil determines a rate of infiltration.

Land surface parametrizations have to represent correctly the surface fluxes and the evolution of soil moisture in all four phases of the cycle, and to switch from the atmosphere control into the soil control regime. The evolution of soil moisture will determine when point D will occur, and the evaporation formulation will determine point B. The crucial areas, from the point of view of the atmosphere, are B-C and C-D. During spring and summer (when the atmospheric evaporative demand is very large), the system stays much longer in the states B-D than in the opposite part of the cycle.

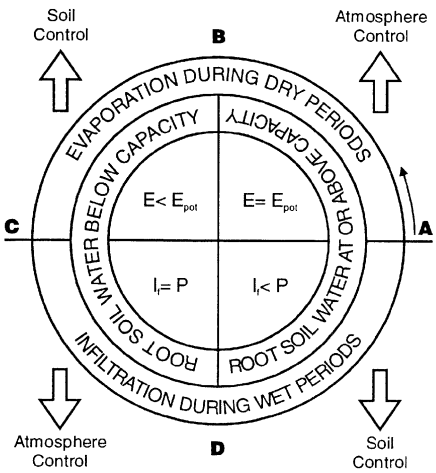

Figure 3. Schematic depiction of the interaction between the soil hydrology and the atmosphere (from Dooge, 1992a).

Before going into further detail, we will present an early example of awareness of the role of the different mechanisms controlling the surface heat and water budget: Richardson (1922), in his classical book on numerical weather prediction, identified practically all the relevant subjects in land surface parameterization. First of all, he notes that lower boundary conditions for the atmospheric equations simplify greatly if one makes a forecast for the soil water content. The surface of the earth is separated in sea, bare ground and vegetated part, and he proposes to use the relative fractions of the above within a grid square. The soil heat budget and water budget are to be solved by discretizing the partial differential equations representing the soil heat transfer and soil water transfer. The depths of the 5 soil layers are in a logarithmic distribution, with a total soil depth of 1.5 m, common to soil temperature and

© ECMWF, 2002

soil moisture (in order to take into account easily the energy exchanges into phase changes in the soil water and the energy transported with the water in the soil).

He is probably the first author to write an equation for the water transfer in the unsaturated part of the soil. The idea of generalising Darcy's law (established in 1856 for the flow of water in a saturated medium) to the flow of water in unsaturated soil, is normally attributed to Richards (1931). In fact, Richardson had done it nine years earlier. He proposes to integrate the resulting partial differential equation with precipitation and evaporation as top boundary conditions, and to specify soil water properties (matric pressure head and hydraulic conductivity) depending on soil water content. Moreover he includes in the soil water balance an additional term representing the effect of transport of water in vapour phase. For soil heat transfer, the classical Fourier law is applied, with heat conductivity depending on soil moisture. Two additional terms are included: the first for the heat transported with the water, the second for the heat involved in phase changes (liquid–vapour) within the soil. The top boundary condition is the net heat flux at the surface, added to the energy content associated with water falling as precipitation.

For computation of the evaporation from a canopy, he recognizes the physiological control of plants in reducing transpiration below a certain threshold value of soil moisture, made dependent on soil type. The notion of canopy resistance, together with its "electrical" analogy, is properly introduced. An interception reservoir is used, representing the leaves, collecting precipitation and evaporating at the potential rate. The bare ground evaporation depends on the relative humidity in the air pores of the top soil layer.

All the principles currently used by most current surface parameterization schemes have been proposed by Richardson in 1922. The way he infers values for the constants involved is reminiscent of current practice, where one value for a particular site is generalized to the whole globe: a noticeable difference is that he performed field experiments in order to estimate parameters or study phenomena for which there was insufficient evidence, e.g., for canopy interception.

Before closing the section, we will present combination equations for estimating evaporation: a special family of equations obtained by simultaneous solution of the surface energy balance and turbulent transport of heat and water vapour, taking into account the internal plant resistance to transpiration. Penman (1948) was the first to obtain such an equation, for an open-water (or well-watered) surface. The introduction of the effect of vegetation (through the stomatal resistance of a single leaf or a canopy resistance for the effect of the entire canopy) gives rise to what is normally called the Penman–Monteith equation. For a review of combination equations, and the different derived forms of the Penman equation, see Brutsaert (1982), Milly (1991), and Monteith (1980, 1981). In the following, a sketchy derivation of the Penman–Monteith equation will be presented. Combination equations are interesting for a number of reasons. First, they are useful for micrometeorological estimates of evaporation, because they eliminate the surface temperature from the surface energy budget. Secondly, they can be used to estimate regional evaporation on a daily or monthly basis (Priestley and Taylor, 1972). Thirdly, they can be used in NWP models (Pan, 1990) as a basis for the surface parametrization. Finally, they are a powerful interpretative tool for analysing experimental or model results and understanding the physical mechanisms responsible for evaporation.

When storage terms in the vegetation are neglected, energy conservation at the interface soil/vegetation/atmosphere implies

$$R_n + G + LE + H = 0 \tag{1}$$

where R_n is the net radiation at the surface (sum of net shortwave, the downward longwave, and the upward longwave emitted by the surface), L the latent heat of vaporisation (sublimation if the water exists at the surface in the solid phase), and G, E and H are the ground heat flux, rate of evaporation, and sensible heat flux, respectively. All fluxes are positive downwards and have units of W m^{-2}. G can also be interpreted as minus the rate of heat

© ECMWF, 2002

storage beneath the surface (vegetation plus soil), in which case (1) represents the heat budget of a finite vertical slab of soil+canopy. Eq. (1) states that all significant water in the soil available for evaporation exists in the liquid (solid) state, the water is transferred to the atmosphere in the vapour state at the expense, energetically, of the surface: the surface provides the latent heat, with a corresponding cooling in case of an upwards moisture flux.

Using Monin–Obukhov similarity, the sensible heat flux can be written as

$$H = \rho C_p C_{\mathrm{H}}(z_{0\mathrm{h}}, z_{0\mathrm{m}}, L) U_L (T_L - T_{\mathrm{sk}}) \tag{2}$$

where ρ, C_p, U, T, $z_{0\mathrm{h}}$ and $z_{0\mathrm{m}}$ are, respectively, the air density, specific heat at constant pressure, wind speed, temperature, roughness length for heat and momentum, the subscript L represents an arbitrary level (at height z_L) within the surface layer, T_{sk} is the skin or canopy temperature, the temperature at a point in the air immediately adjacent to the canopy (or the soil, in case of bare ground). C_{H} is the exchange coefficient for heat and L is the Obukhov length; a functional form of C_{H} can be found, e.g., in Beljaars and Holtslag (1991). Eq. (2) can be rewritten in resistance form,

$$H = \rho C_p \frac{T_L - T_{\mathrm{sk}}}{r_{\mathrm{a}}} \tag{3}$$

By comparing (2) and (3), we obtain

$$\frac{1}{r_{\mathrm{a}}} = C_{\mathrm{H}} U_L \tag{4}$$

relating the aerodynamical resistance, r_{a}, to the product of the wind speed and the exchange coefficient for heat.

The evaporation flux, the flux of water between the air inside the stomata, at saturation, and the air in the surface layer can be modelled following (3). We have now conceptually two resistances, one from the air inside the stomata up to the surface of the leaves, r_{s}, and the second one from the surface of the leaves up to level z_L r_{a}

$$E = \rho \frac{q_L - q_{\mathrm{sat}} T_{\mathrm{sk}}}{r_{\mathrm{s}} + r_{\mathrm{a}}} \tag{5}$$

where q_L and q_{sat} are the specific humidity at level z_L and the saturation specific humidity, respectively. By assuming the same aerodynamical resistance for heat and water transfer, we are implicitly assuming identical roughness lengths for heat and moisture.

Assuming we can specify r_{a} (standard turbulence estimates, using Eq. (4)) and r_{s} (from the knowledge of canopy state and canopy type, and other environmental factors) and have an estimate for q_L (standard SYNOP observation or lowest model level value). Eq. (5) has still one unknown T_{sk}. By performing a Taylor expansion of $q_{\mathrm{sat}}(T_{\mathrm{sk}}) - q_{\mathrm{sat}}(T_L)$, $T_{\mathrm{sk}} - T_L$ can be eliminated by using Eqs. (1) and (3). If we retain the linear term in the expansion (see Milly, 1991, for higher order approximations), use the Clausius–Clapeyron equation for the slope of the saturation specific humidity function, $S = \mathrm{d}q_{\mathrm{sat}}/\mathrm{d}T\big|_{T=T_L}$, the Penman–Monteith equation is finally obtained:

$$-LE = \frac{\rho \dfrac{C_p}{r_{\mathrm{a}}} [q_{\mathrm{sat}}(T_L) - q_L] + S(R_{\mathrm{n}} + G)}{\dfrac{C_p}{L}\left(1 + \dfrac{r_{\mathrm{s}}}{r_{\mathrm{a}}}\right) + S} \tag{6}$$

© ECMWF, 2002

Evaporation is driven by a combination of two terms, the first proportional to the saturation deficit at screen level height (the advection term), and the second proportional to net radiation minus the soil heat storage (the energy term). During day time summer G is small compared to R_n for a vegetated area (typical instantaneous midday values are 80 W m^{-2} and 600 W m^{-2}, respectively) and can either be neglected or made proportional to R_n. In winter, $(R_n) + G$ and S are small and the saturation-deficit term dominates. If we also have an unstressed canopy, r_s takes its minimum value, and evaporation depends crucially on the aerodynamical resistance (the combined effect of stability and roughness length). Typical values of aerodynamical resistances are (see Shuttleworth, 1993b) 45 s m^{-1}, 18 s m^{-1}, and 6.5 s m^{-1} for grassland, agricultural crop and forest, while the minimum (unstressed) stomatal resistance varies from a value of 60 s m^{-1} over grassland to 120 s m^{-1} over forest. The fact that smaller values of r_s are associated with larger values of r_a makes the first term in the denominator of (6) to change significantly between grassland and forest; with the numbers given above, it will vary by a factor of 10.

Using Eq. (6), we can now quantify some of the different idealized evaporation concepts presented earlier in this section. *Potential evaporation* is obtained when there in a well watered surface or a wet canopy $(r_s) = 0$. It corresponds to the maximum possible value of evaporation; note also that T_L has to be replaced by the value that it would assume when the surface is wet (see below). *Unstressed evaporation* (or *potential evapotranspiration*) is obtained by replacing r_s by its minimum value: the effect of the canopy even in unstressed conditions can modify the first term in the denominator by a factor of 10, therefore making, e.g., forest unstressed transpiration substantially smaller than potential evaporation.

Pan (1990) used Eq. (6) as basis for the parametrization of evaporation in the NMC global model. Unstressed evaporation is computed using a modified temperature T'_L characteristic of a well wet surface; note that T'_L changes the value of the advection term and the radiative term (through the thermal radiation emitted by the surface). A practical way of computing the effects of T'_L is based on Taylor expansions of both terms. Actual evaporation is computed as the product of an evaporative fraction, β, times unstressed evaporation.

To summarize, the Penman–Monteith equation stresses that: (i) evaporation is driven by two large environmental factors, an energy capping given by the net radiation, and an "advection" factor given by the saturation deficit term; (ii) the rate of evaporation is controlled by the nature and state of the surface cover, given by the ratio r_s/r_a, the presence of r_s indicating the physiological control by the plants.

3. SOIL ENERGY AND WATER BUDGET

3.1 Soil energy transfer

Neglecting the coupling of water transfer in the soil with the heat transfer, we can assume the following Fourier law of diffusion to govern the soil heat transfer

$$(\rho C)_s \frac{\partial T}{\partial t} = \frac{\partial}{\partial z}\left[\lambda_T \frac{\partial T}{\partial z}\right] \tag{7}$$

where $(\rho C)_s$ is the volumetric soil heat capacity (J m^{-3}K^{-1}), T is the soil temperature (K), z is the vertical coordinate (distance from the surface (m), positive downwards), t is time (s), and λ_T is the thermal conductivity (W m^{-1}K^{-1}). In Eq. (7), the heat transfer is assumed to occur only in the vertical direction.

The volumetric heat capacity and the thermal conductivity depend on the soil type and its water content, and therefore we will shortly review here general properties of soils. For more details on descriptive information on soil science see, e.g., Hillel (1982), Duchaufour (1984), Marshall and Holmes (1988). The soil is a three phase heterogeneous system, where the solid phase is called the soil matrix, the liquid phase is the soil water and the gaseous

© ECMWF, 2002

phase is the moist air trapped in its pores (Hillel, 1982). The soil phase includes the mineral matter and, in some cases, organic matter attached to the mineral grain and binding them together. The fraction of soil occupied by the soil pores is called porosity, or volume of air trapped over total volume, θ_s (m^3m^{-3}). θ is the symbol used here for soil wetness, and s the subscript for saturation. Indeed porosity coincides with the total amount of water that can be held by the soil in its pores (saturation soil wetness). Porosity of most soils is of the order of 0.5 m^3m^{-3}, except for soils with high organic content, e.g., peat, where values as high as 0.8 m^3m^{-3} can be found.

The soil is characterized by its texture (the size distribution of the soil particles), structure (the spatial organization of the soil particles), composition (the types of minerals existent in the soil), and water content. For heat and moisture transfer, the most relevant variables are water content and texture, the former modulating the intensity of heat and moisture fluxes, while the latter determines essentially the amount of water that the soil can hold against the combined effects of gravity and pressure (see next section). In terms of texture, any given soil is normally characterized by its percentage of clay, silt and sand. For the purposes of classification, the United States Department of Agriculture (USDA) has defined a textural triangle, each side corresponding to a type of particles, sand, silt or clay. Any particular soil becomes a point inside this triangle, according to its texture. Areas within the triangle become soil types. USDA defines eleven soil types, ranging from the finer textures (clay), through the intermediate textures (loam), and coarser textures (sand).

In order to integrate Eq. (7) one needs to specify values for its coefficients. The soil heat capacity can be estimated as an weighted sum of the heat capacity of its phases (de Vries, 1963, 1975). The air heat capacity being three orders of magnitude smaller than the other phases, we can write

$$(\rho C)_s = (1-\theta_s)(\rho C)_m + \theta_m(\rho C)_w \tag{8}$$

where the subscript m and w refer to the soil matrix and water respectively. $(\rho C)_m$ ranges from 2×10^6 J $m^{-3}K^{-1}$ for most minerals, up to 2.5×10^6 J $m^{-3}K^{-1}$ for organic matter. Because $(\rho C)_w$ is 4.2×10^6 J $m^{-3}K^{-1}$, typical values for $(\rho C)_s$ are around 3×10^6 J $m^{-3}K^{-1}$, and vary by a factor of two depending on its water content. For a frozen soil, Eq. (8) can be modified to

$$(\rho C)_s = (1-\theta_s)(\rho C)_m + \theta_w(\rho C)_w + \theta_i(\rho C)_i \tag{9}$$

where θ_w and θ_i stand for the liquid and ice water content of the soil, respectively and $(\rho C)_i = 1.9\times10^6$ J $m^{-3}K^{-1}$. Thermal conductivity depends not only on soil texture and water content, but also soil structure. de Vries (1975) developed a general theory, that can be used for a given soil in the field, but inadequate (too detailed) for application to large scale modelling. A simple expression in terms of water content and soil type can be found in McCumber and Pielke (1981). For a medium texture soil (loam, type 5 on the USDA classification), values range from 0.428 W $m^{-1}K^{-1}$ for a dry soil up to 2.24 W $m^{-1}K^{-1}$. Values for coarser (sandy soils) can be twice as large.

A complete theory of heat and moisture transfer must describe the moisture transfer under the combined influence of gradients of temperature and moisture content (see next section), and the heat transfer under the influence of temperature gradients and mass flow of moisture. The theory has been developed by Philip and de Vries (1957) and de Vries (1958), and further generalized by Milly (1982), in the presence of hysteresis, but it is not in use by current GCM parametrizations. In practice Eq. (7) can be used for all cases, provided (9) is used for the heat capacity, and some other relation is used to define heat conductivity in terms of soil wetness. A notable exception is the treatment of frozen soils. In the absence of snow cover, a soil that is cooling from, say 5 C, up to the freezing temperature will stay at a constant temperature, around 0 C, during a couple of weeks (see Williams and Smith, 1992, and Verseghy, 1991), and afterwards will continue its cooling. This corresponds to heat released by the phase change of the water in the soil into ice: until the whole water in the soil column is frozen, any further radiatively driven cooling will not produce lower soil temperatures. This is a common phenomenon in high latitudes during

© ECMWF, 2002

the autumn and early winter; the reverse mechanism, when the soil is thawing in spring, holds the temperature close to 0 C for much longer than Eq. (7) would predict. If a model does not consider phase changes of water, and their impact on the heat budget, the near soil temperature will reveal a cold bias during the freezing in the autumn, and a warm bias in spring thawing - the warm bias will be less common, because the soil will typically be covered with snow, acting as an insulator layer.

The top boundary condition for the integration of Eq. (7) is of the flux form, the net heat flux at the soil/atmosphere interface. At the bottom, the boundary condition can be given (a) as a no-flux boundary condition (if the soil is deep enough), (b) by specifying a seasonal heat flux at the bottom, or (c) specifying a seasonally varying temperature at the bottom. In practice, for integration of Eq. (7) one needs to discretize in space and time. Discretization in space means choosing soil layers of a given depth, each layer will be characterized by its thermal inertia (Warrilow *et al*., 1986), the upper layers changing more rapidly than the lower layers (see also Dickinson, 1988).

3.2 Soil water transfer

The movement of water in the unsaturated zone of the soil obeys the following equation

$$\rho_w \frac{\partial \theta}{\partial t} = -\frac{\partial F}{\partial t} + \rho_w S_\theta \tag{10}$$

where θ_w is the density of water (kg m^{-3}), $\boldsymbol{F}$ is the water flux in the soil (postive downwards, kg $m^{-2}s^{-1}$), and S_θ is a volumetric source term ($m^3m^{-3}s^{-1}$), corresponding to root extraction (the amount of water transported from the root system up to the stomata - due to the difference in osmotic pressure - and then available for transpiration), and phase changes of ice to liquid water. Eq. (10) assumes that horizontal transfers are negligible, which holds for a grid box of 50×50 km: for much smaller scales, local terrain slope can induce large horizontal water fluxes.

As seen in Section 2, Richardson (1922) and Richards (1931) extended Darcy's law to the flow of water in the *unsaturated* case, expressing the water flux in terms of a gradient of the hydraulic head, a sum of matric head, ψ (units m of water), and gravitational potential,

$$F = -\rho_w \left[\gamma(\psi) \frac{\partial \psi}{\partial z} - \gamma(\psi) \right] \tag{11}$$

Once more we are neglecting lateral gradients of $(\psi - z)$ in the mechanisms responsible for water transfer. The matric head is homogeneous (has the same units) to the symmetric of pressure p, and $g(\psi - z)$ can be interpreted as an energy per unit mass, or the work necessary to extract from the soil a unit mass of water against capillarity and gravity. The hydraulic conductivity γ (m s^{-1}) is a function of the pressure head. In order to integrate (10) with the flux definition (11), an expression is needed for $\psi = \psi(z)$, or, alternatively, $\psi = \psi(\theta)$. Such an expression would allow us to write

$$F = -\rho_w \left[\gamma(\theta) \frac{\partial \psi}{\partial z} - \gamma(\theta) \right] \tag{12}$$

$$\lambda = \gamma \frac{\partial \psi}{\partial \theta} \tag{13}$$

Hysteresis effects mean that γ is neither a unique function of ψ or θ. Defining the hydraulic diffusivity, λ (m^2s^{-1}), as $\lambda = \gamma(\partial\psi/\partial\theta)$, (12) can be rewritten as

© ECMWF, 2002

$$F = -\rho_w\left[\lambda(\theta)\frac{\partial\theta}{\partial z} - \gamma(\theta)\right] \tag{14}$$

Combining (14) with (10), we obtain

$$\frac{\partial\theta}{\partial t} = \frac{\partial}{\partial z}\left[\lambda\frac{\partial\theta}{\partial z}\right] - \frac{\partial\gamma}{\partial z} - S_\theta \tag{15}$$

Eq. (15) with a zero source term is normally called Richards equation. Neglecting the second and third term in the r.h.s., Eq. (15) looks like a Fickian equation for diffusion. Hillel (1982) cautions against pushing too far this analogy, because the process modelled by Eq. (15) is not molecular (or turbulent) diffusion but water transfer through a porous media. The other difference between (15) and (7), of a more practical nature, is in the forcing (Savijärvi, 1992): the heat flow equation in the soil is forced in spring and summer mainly by net radiation at the surface, a sum of harmonics corresponding to the diurnal and the seasonal forcing modulated by the presence of cloudiness. In contrast, the forcing of (15) at the surface is the quasi-random signal of precipitation.

Integration of Eq. (15) needs functional relationships for $\lambda = \lambda(\theta)$ and $\gamma = \gamma(\theta)$. Hillel (1982) reviews several empirical equations proposed, and Mahrt and Pan (1984) compared an extensive set of measured relationships for different textures. They all obey the functional form (Clapp and Hornberger, 1978, Cosby *et al.*, 1984)

$$\begin{aligned}\gamma &= \gamma_{sat}\left(\frac{\theta}{\theta_{sat}}\right)^{2b+3}\\ \lambda &= \lambda_{sat}\left(\frac{\theta}{\theta_{sat}}\right)^{b+2}\end{aligned} \tag{16}$$

where γ_{sat} and λ_{sat} are the values at saturation of hydraulic conductivity and diffusivity, respectively, and b is a non-dimensional coefficient, called the Clapp and Hornberger exponent. Note that Eq. (16) indicates a stronger variation in terms of soil moisture for conductivity than diffusivity, with twice as many orders of magnitude covered. Clapp and Hornberger and Cosby *et al.* measured values for γ_{sat} and λ_{sat} for a very large sample of soils classified in the eleven soil classes of the USDA classification. The three coefficients vary widely over the textural classes: (i) γ_{sat} varies between 1×10^{-4} and 1.76×10^{-2} m s^{-1} between coarser textures (sand) and finer textures (clay), respectively; (ii) λ_{sat} varies between 8.22×10^{-5} m^{2}s^{-1} and 2.18×10^{-2} m^{2}s^{-1}, between coarser and finer textures; (iii) b values range from 2.8 to 11.5 for coarser and finer textures, respectively. For a given soil type, variations in terms of soil moisture are even more dramatic. For a medium texture soil (loam), γ varies between 1.07×10^{-10} m s^{-1} and 1.48×10^{-6} m s^{-1} for a range of acceptable values of soil moisture from a dry soil to a wet soil, respectively; λ for the same soil moisture values is 5.77×10^{-7} m^{2}s^{-1} and 9.29×10^{-5} m^{2}s^{-1}, respectively.

The non-linear variations of λ and γ in terms of soil moisture makes Eq. (15) (or its counterpart expressed in $\boldsymbol{y}$ terms) difficult to integrate, even numerically. Wang (1992) reviews analytical solutions of the Richards equation for some simple representative cases covering each of the four quadrants of the hydrological rosette (Fig. 3), with very idealized formulations for precipitation, evaporation and the recharge flow as lower boundary condition (see also Eagleson, 1978a). Boundary conditions for Eq. (15) are, at the top, infiltration (that part of precipitation that is available to wet the soil, i.e., precipitation minus surface runoff minus interception) and, at the bottom, the flow of water from underneath. Two lower boundary conditions can be envisaged (Abramopoulos *et al.*, 1988), corresponding to the two limit cases of bedrock or no bedrock underlying the soil domain, the former specifying F as its drainage (γ) part, while the latter corresponds to a zero water flux. Some authors (see e.g., Wang, 1992, Dümenil and Todini, 1992) include in the lower boundary condition a base flow, mimicking the effect of lateral subterranean flow, as well as vertical water loss.

© ECMWF, 2002

From all generalizations to equation (15) (see Philip and de Vries, 1957; Philip, 1957; Milly, 1982), there are two of items of relevance for large scale atmospheric models. The first one relates to the inclusion of water vapour. For arid regions, the soil vertical transfer in the upper few cm is driven by variations of the water vapour in the soil pores (for a more detailed discussion see Subsection 3.3 below). However, because this transfer occurs in a very shallow top layer, a vertical resolution typical of current parameterization schemes prevents its explicit consideration. Mahrt and Pan (1984) proposed a parameterized way of dealing with it. The second deals with the inclusion of the solid phase of water, essential for modelling the soil water transfer in high latitudes. Its is possible to write additional equations for the conservation of frozen water at different soil layers (Verseghy, 1991, Pitman *et al*., 1992). An alternative way to deal with it is to specify the percent of soil water in the frozen state, in terms of temperature, and to specify its effect on soil water transfer in terms of a frozen water matric potential (Peter Cox, personal comm., Black and Tice, 1988, Williams and Smith, 1992, Miller, 1980). The latter approach avoids the use of additional prognostic variables, but requires the same vertical discretization for soil moisture and temperature. The term S_θ in that case will include melting/freezing effects, with an equivalent term for the energy equation. Proper consideration has to be given to the root extraction term, in order to make it ineffective in the presence of frozen soils: in boreal forests this retards the beginning of significant evaporation until late May or June when the whole column of the soil is thawed, long after the solar radiation starts to increase (Sellers *et al*., 1995).

3.3 Boundary conditions

3.3 (a) Surface sensible heat flux. A way of defining the sensible-heat flux has already been presented in Eq. (2), including the dependency on atmospheric stability and the consideration of different roughness lengths for heat and momentum. Many versions of Eq. (2) have been presented recently in the literature and the reader is referred to Dyer (1974), Garratt (1992), Högström (1988), and Stull (1988) for details. We will mention here only a couple of relevant points. Beljaars (1995) include in the definition of velocity a convective velocity scale, or free convection velocity, w_*, characterizing the intensity of turbulence in well mixed unstable boundary layers. Its inclusion ensures a proper asymptotic limit of the stability dependent functions in case of free convection. The skin layer temperature, T_{sk}, can also be used a temperature representative of the surface. The skin layer temperature is representative of a infinitesimally thin layer with zero heat capacity, isolating the underlying soil from the radiative heating above. The use of the skin layer, instead of the average soil temperature characteristic of the top few cm in the soil, reduces the ground heat flux amplitude and phase errors, and the phase error in the diurnal cycle of sensible and latent heat flux (Betts *et al*., 1993). If an average soil temperature is used, the depth of the soil represented by that temperature has to be warmed, for the temperature to rise in response to the radiative forcing, introducing a phase lag of 1–2 hours between the peak of radiative forcing and the peak of the top soil temperature (Beljaars and Betts, 1993).

Most GCMs do not distinguish the roughness length for heat and momentum. However, the mechanisms responsible for drag are related to bluff body effects, and are more efficient than the conduction at the interface through which the heat transfer is performed. Brutsaert (1982) presents abundant experimental evidence for the difference between the two roughness lengths, while Beljaars and Viterbo (1994) show the impact of properly separating the two values onto spring systematic errors on near surface humidity over well wet mid-latitude areas (Cabauw, the Netherlands). The problem is more serious in GCMs because roughness lengths are order of magnitudes larger than their micrometeorological values (see Mason, 1988, 1992), where the necessary compensating decrease of the roughness for heat is hardly ever used. A stability formulation in terms of z/L allows a direct use of measured stability functions, and an easy way of separating heat and momentum roughness length. The disadvantage is the need to solve a non-linear equation for every time step expressing the Obukhov length in terms of the bulk Richardson number. A stability formulation in terms of a Richardson gradient number, for $z_{0\mathrm{m}} \neq z_{0\mathrm{h}}$ is presented in Mascart *et al*. (1995).

© *ECMWF, 2002*

3.3 (b) Evaporation . Formally, an equation analogous to (2) can be written for the evaporation,

$$E = \rho C_H \|U\| [\alpha_L q_L - \alpha_s q_{sat}(T_{sk}, p_s)] \tag{17}$$

where α_L and α_s are factors dependent on the soil cover and state, vegetation type and phenological state, environmental factors like radiative forcing and humidity saturation deficit at the surface: $\alpha_L, \alpha_s < 1$. The first approach for specifying evaporation in a GCM was given by Manabe (1969) based on the concept of "evaporative factor" β (Budyko, 1974). In our notation, that corresponds to

$$\alpha_L = \alpha_s = \beta = \min\left(1, \frac{\theta}{\theta_{max}}\right) \tag{18}$$

where θ and θ_{max} are the actual and maximum contents of a single reservoir of water (bucket) in the soil. A separate prognostic equation for q is needed for the definition of (18) at every time step. Milly (1992) discusses the proper use of (17) and (18); as mentioned earlier, in some cases a different equilibrium temperature, T_{eq}, characteristic of the conceptual irrigated surface, is needed, defined as $\alpha_s q_{sat}(T_{sk}) = \beta q_{sat}(T_{eq})$, and compatible with Budyko's notion of evaporative fraction and potential evaporation.

The bucket model is inadequate for a number of reasons. First, the use of only one layer in the soil (a single soil reservoir) does not allow a quick response to precipitation events. For bare soil, it is an observational fact that, after a very brief period at the potential rate, evaporation is greatly reduced after the loss of water in the first few cm of the soil (representing at most 1 cm of water). The bucket model overestimates bare soil bare soil evaporation in almost all regimes. For vegetated areas, the bucket model fails to recognized the impact of the canopy resistance on evaporation. For unstressed vegetation, the bucket model gives potential evaporation ($r_s = 0$), instead of unstressed evaporation (minimum, non-zero, value of r_s), as an estimate for real evaporation. As discussed before, this will produce a significant over-estimation of transpiration: this leads to overevaporation following a precipitation event, producing a rapid drying of the soil and, afterwards, too small evaporation because there is not enough water available in the soil for evaporation. For that reason, a number of alternative methods exist to estimate evaporation in GCMs, and in the following sections we will present their physical/physiological basis.

1) Canopy evaporation

The canopy evaporates due to two different mechanisms. The wet part of the canopy, covered by a thin film of water, shortly (a few hours) after a precipitation event or deposition of dew, evaporates at the potential rate (Deardorff, 1978); note that this can be substantially larger than the unstressed transpiration, hence the interest in the distinction. In our notation $\alpha_L = \alpha_s = 1$. The role of surface parametrization in this case is to establish the fraction of the canopy that is wet, and to have a predictive equation for the intercepted water, in order to establish how long the canopy can evaporate at the potential rate.

For dry canopy, most of the current parametrization schemes use the so-called "big leaf-big stomata" (Monteith, 1965) approach. These models recognize that plants evaporate due essentially to a two-path mechanism:(i) the first, physiologically controlled, transports water from the root zone up to the stomatal cavities, where water vapour is at saturation; (ii) the second, aerodynamically (environmentally) controlled, transports water from the stomata up to the air in the surface layer. Plants regulate evaporation by controlling the aperture of the stomata. In a steady state, the aperture of the stomata is the mechanism that controls the root water upflow, and is enough to characterize the whole physiological control of evaporation. In most species, stomata regulate the outflow of water vapour and the intake of carbon dioxide for photosynthesis; the energy

© ECMWF, 2002

required for opening and closing the stomata, and for the uptake of the root zone soil water is provided by radiation (photosynthetically active radiation, PAR, mainly the visible part of shortwave radiation, roughly 55% of the total shortwave). Under most environments, the system appears to operate in such a way as to maximize the carbon dioxide intake for a minimum water vapour loss. When soil moisture is scarce, the stomata close to prevent desiccation of the plant.

The integrated behaviour of the whole canopy can be conceptually represented by the schematic resistance diagram of Fig. 4 (from Dickinson *et al.*, 1991). The right hand side represents the sensible heat transfer, while the left hand side represents evaporation. The equation corresponding to such a resistance network is

$$E = \rho \frac{q_L - q_c}{r_a + r_c} = \rho \frac{q_L - q_{sat}(T_{sk})}{r_a + r_c} \tag{19}$$

where q_c is the specific humidity in the stomata cells. The canopy resistance is the integral mean of the resistance of the individual leaves, assumed to act in parallel (Dickinson *et al.*, 1991):

$$r_c = \frac{\langle r_s \rangle}{L} \tag{20}$$

where the brackets represent a leaf-area inverse average (conductances, $1/r_s$, are linearly averaged)

$$\langle (\,) \rangle = \frac{L}{\int_L \frac{dL}{(\,)}} \tag{21}$$

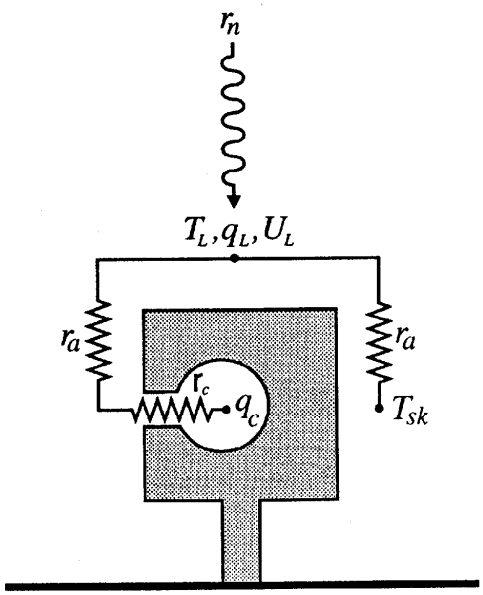

Figure 4. Schematics of the surface transpiration resistance.

© ECMWF, 2002

The quantity measured for a single plant is the stomatal resistance, r_s. Most of the atmospheric models use the multiplicative approach of Jarvis (1976), to express the surface resistance as a product of a minimum factor times a number of limiting factors

$$r_s = r_{smin} f_1(PAR) f_2(\theta) f_3(T) f_4(D) \tag{22}$$

where $f_i^{-1} < 1$, and D is the vapour-pressure deficit at the air surrounding the leaves. Typically, f_1^{-1} varies between 0 with no insolation and 0.9 at 200 W m^{-2} (Dickinson *et al.*, 1991, Sellers, 1985). f_3^{-1} has a bell-like shape, peaking at some (species dependent) optimal temperatures T_{op}, and close to 0 for too-low or too-high temperatures. The saturation deficit conductance function, f_4^{-1}, is a dominant mechanism for forests, but unimportant for grassland.

The dependence on soil wetness is implemented differently for almost every surface parametrization scheme. θ represents a measure of the water in the root zone, which is typically the top 1 m of the soil, but varies with ecological type:(i) It is shallower (around 0.5 m) for crops which, being "man-nurtured" have a less adaptive nature; (ii) Around 1 m for mid-latitude and boreal forests; (iii) several metres (up to 10 m) deep for savannah-like vegetation; and iv) only 0.5 m for the trees of equatorial forests. A map of the depth of the root zone can be found in Patterson (1990).

All models shut evaporation ($f_3^{-1} = 0$) below a critical point, θ_{pwp} the permanent wilting point, or the *value at which plants can no longer recover turgidity even when placed in a saturated environment* (Hillel, 1982). Being related to the energy involved in the transport of water up to the root zone, the permanent wilting point corresponds to a very large value of the matric potential, ψ. A value of $\psi_{pwp} = 153$ m (15 bar) is widely accepted as characteristic value for most soils. Based on Cosby *et al.* (1984) estimates, it is possible to obtain θ_{pwp} for each soil type of the USDA classification. Values range from 0.033 m^{3}m^{-3} for coarser sandy soils, up to through 0.145 for loamy intermediate soils, and 0.25 for finer soils. Patterson (1990) presents a critical review of the experimental estimates of θ_{pwp}.

All models have a stress-free evaporation ($f_3^{-1} = 1$) beyond a critical point which is a fraction of the field capacity; the fraction should lie in the range 0.5 to 0.8 (Shuttleworth, 1993b), but in parametrization schemes ranges between 0.7 and 1. The field capacity is the maximum amount of water an entire column of soil can hold against gravity, or the *equilibrium mean value of a column soil water 24–48 hours after wetting the soil* (Hillel, 1982). Having such a "loose definition", it is not surprising that estimates of field capacity for one particular soil type vary so widely. Hillel (1982) discusses the problems associated with the concept and use of field capacity, and Patterson (1990) reviews experimental estimates for different types of soil. It is common to associate field capacity to a certain value of hydraulic conductivity, with values ranging from 0.05 mm d^{-1} to 0.1 mm d^{-1} (Warrilow *et al.*, 1986, Eagleson, 1970, Jacquemin and Noilhan, 1990): the value of θ_{cap} can be estimated in this way from Eq. (19). These estimates give generally too small a value of field capacity, and an alternative quantitative way of defining it is to assign a certain value of ψ, ranging from 1 m (0.1 bar) to 3.4 m (0.33 bar). Patterson (1990) concludes that no single value of ψ_{cap} is appropriate for every soil texture. A value of 3.4 m overestimates ψ_{cap} for fine textures and underestimate it for coarse textures. Estimated values of θ_{cap} range from 0.093 through 0.288 up to 0.384 m^{3}m^{-3}, for coarse, medium, and fine texture soils, respectively. Given that evaporation is zero below θ_{pwp} and at the unstressed rate above θ_{cap} the availability, or available water capacity, θ_{ava} defined as

© *ECMWF, 2002*

$$\theta_{ava} = \theta_{cap} - \theta_{pwp} \tag{23}$$

is a very important quantity (Patterson, 1990, Henderson-Sellers *et al*., 1993). When multiplied by the root depth, it gives the total amount of water available for evaporation or total water holding capacity (units m of water): this quantity determines the size of the reservoir and, as such, is crucial in determining time constants in long drying periods. A geographical distribution of total water holding capacity is given by Patterson (1990).

The different ways of applying f_3^{-1} relate to the shape of the curve linking the 0 and 1 branches. Some authors have a linear dependency in ψ (Abramopoulos *et al*., 1988; Federer, 1979), while others have linearity in θ (Warrilow *et al*., 1986; Noilhan and Planton, 1989; Blondin, 1991). The other difference lies in the specification of θ in multilevel models: (i) It can be taken as a weighted average value over the root zone, with the weights proportional to the root profile (Blondin, 1991); (ii) It can be taken as the minimum value of the soil moisture in the root zone (Abramopoulos *et al*., 1988), the water is borrowed from where it is "energetically cheaper"; and iii) f_3^{-1} is a product of corresponding values for each root layer (Federer, 1979). A large uncertainty exists to what method is a better representation of nature.

2) Soil (bare ground) evaporation

As illustrated schematically by Fig. 5 (from Mahfouf and Noilhan, 1991), soil (bare ground) evaporation is due to a combination of two physical processes (Kondo *et al*., 1990, Mahfouf and Noilhan, 1991): (i) Molecular diffusion from the water trapped in the pores of the soil matrix up to the surface/atmosphere interface, defined by the humidity roughness length, z_{0q} (Brutsaert, 1982); (ii) Laminar and turbulent exchange in the air between z_{0q} and screen level height (e.g. 2 m above z_{0q}). Process (ii) can be characterized by the atmospheric resistance, r_a, defined by Eq. (4). Process (i) involves a soil resistance, r_{soil}, and is dependent on relative humidity adjacent to the free-water surface in the soil matrix. The humidity equilibrium value can be expressed by an exact thermodynamic relationship in terms of soil temperature close to the pores (Philip, 1957). In dry situations the relative humidity in the pores has a strong vertical gradient in the top few mm of the soil. r_{soil} is inversely proportional to the diffusivity of water vapour, and strongly dependent on soil texture and structure (Kondo *et al*., 1990). An accurate description of bare soil evaporation can be obtained with a soil model with circa 10 layers in the top 5 cm of the soil, in order to model explicitly the diffusivity of water vapour (McCumber and Pielke, 1981, Sasamori, 1970, Camillo *et al*., 1983). The small time step required in such a model makes its cost prohibitive for large scale problems. The depth of the first soil layer in GCMs is typically a few cm, too coarse to define explicitly the water vapour transfer.

© ECMWF, 2002

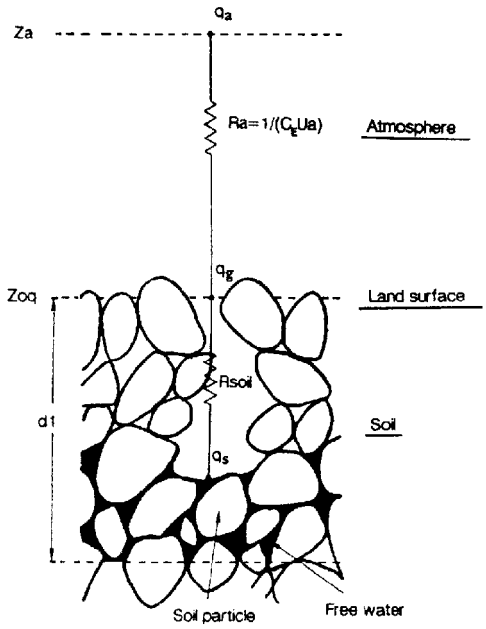

Figure 5. Schematic illustration of the interaction between the atmosphere and a bare soil.

Mahfouf and Noilhan (1991) made a comparative study of several formulations of evaporation over bare ground. Given the above description it is not surprising that most methods reviewed are very sensitive to the top soil discretization of NWP models. The methods presently available were classified in bulk parametrization approaches (α-type and β-type, following Kondo *et al.*, 1990) and threshold methods.

α-methods model the evaporation as a bulk transfer of water vapour between z_{oq} (assumed to be at relative humidity α) and a reference height, typically the height of the lowest model layer. They correspond, in Eq. (22), to $a_L = 1$, $a_s = \alpha$. α can assume several parametrized forms (see e.g., Noilhan and Planton, 1989 and Barton, 1979), depending on the soil water typically in the top 5 cm of soil. In β-methods the evaporation is a fraction β times the bulk transfer of water vapour between the air trapped in the soil pores close to the water in the soil and the reference height. β can be related to a resistance, r_{soil}, for the transfer of water between the soil pore and z_{0q}, and is dependent on the availability of water in the top soil layer (see e.g. Deardorff, 1978, Dorman and Sellers, 1989). The β-method requires the specification of the relative humidity, h, of the air trapped in the soil pores according to Philip (1957) formula (and different from α, relative humidity at z_{0q}). It corresponds, formally, to a rewriting of Eq. (5), with the stomatal resistance replaced by r_{soil}, and $q_{sat}(T_{sk})$ replaced by the specific humidity in the soil pores. Using the notation of Eq. (17), $a_L = 1/(r_a + r_{soil})$, $a_s = h/(r_a + r_{soil})$.

In threshold formulations evaporation proceeds at potential rate above a certain amount of soil water. In drying conditions, when the soil water is depleted, evaporation is determined by the water flux from below (see Mahrt and Pan, 1984, Wetzel and Chang, 1987, Abramopoulos *et al.*, 1988). The evaporation is given by

© ECMWF, 2002

$$E = \min\left\{E_t, \frac{\rho}{r_a}[q_{sat}(T_{sk}) - q_a]\right\} \tag{24}$$

where E_t specifies a maximum water flux from below. In Eq. (24) the first term in the r.h.s is the soil limited evaporation (regime of soil supply in Fig. 3), while the second term is the atmospheric demand term. E_t can be specified in several ways, e.g., the hypothetical water flux between the centre of the top soil layer and the surface assumed at θ_{pwp} (Mahrt and Pan, 1984), who noted that the threshold method depends on the estimation of the soil water flux in a top layer of depth d , and is highly sensitive to the value of d .

The main conclusions of Mahfouf and Noilhan (1991) can be summarized as follows. Threshold methods are very sensitive to the specification of the depth of the top soil layer, where the diurnal cycle is felt, and provide neither a correct diurnal cycle of evaporation, nor the correct transition (on weekly timescales) between the regime of atmospheric demand and the regime of soil supply. α - and β -methods give results of similar quality at day time. During night time, special care has to be taken in order to handle correctly the dew deposition: the two methods give differences in cumulative evaporation of up to 20%.

3.3 (c) Interception. The role of vegetation in intercepting precipitation and collecting dew is a relatively old subject in the meterological literature. Horton (1931) established statistical relationships, valid for monthly periods, between measured net rainfall reaching the ground and over the canopy. Parallel to the statistic estimates of interception (the difference between the rainfall over the canopy and the net rainfall reaching the ground), physically based models of the interception reservoir have been developed, starting with the work of Rutter *et al*. (1972, 1975). Those models evolved from a bulk representation of the canopy into multi-layer plant models (Sellers and Lockwood, 1981). Multi-layer canopy models are too detailed to be coupled with GCMs, but the basic mechanisms of the bulk representation of vegetation have been incorporated into many land surface parametrization schemes (Deardorff, 1978, Dickinson *et al*., 1986, Sellers *et al*., 1986, Xue *et al*., 1991, Noilhan and Planton, 1989, Blondin, 1991). For a review of suitable interception models for coupling with atmospheric models see Mahfouf and Jacquemin (1989). They do not include a proper treatment of interception of snowfall: see Miller (1967) for a discussion of snowfall interception.

All interception models obey the following equation for the evolution of the grid box estimate of the canopy water content, W_l (m)

$$\rho_w \frac{\partial W_l}{\partial t} = a_P P^* + a_l(E_l + D) = I + a_l E_l \tag{25}$$

where all quantities are positive downwards. P^* (kg m^{-2}s^{-1}) is a modified precipitation rate at the top of canopy level, taking into account the subgrid scale distribution of precipitation, $a_l E_l$ is the evaporation coming from the interception reservoir (or wet evaporation), D (kg m^{-2}s^{-1}) is a rate of drainage from the canopy (it is a sink term in the equation, $D \le 0$), and E_l (kg m^{-2}s^{-1}) is the evaporation rate of the wet fraction of the grid box, defined as the potential evaporation rate. a_P and a_l are non-dimensional factors expressing, respectively, the efficiency of interception and the percent of the grid box covered by the interception reservoir (wet fraction). $a_P P^* + D$ is the interception of rain by the canopy, I (kg m^{-2}s^{-1}). $P - I = P - a_P P^* - D$ is called throughfall, all "rainfall" that is available at the ground level. Some authors separate drainage into dripping from the canopy and stemflow, but we will ignore the distinction here. Because the total size of the interception reservoir is very small (0.1–1 mm), interception has to balance wet evaporation on a daily timescale. Note that when $P = P^*$, or $a_P = 1$, the absolute value of throughfall and drainage are identical. What distinguishes any individual model is the specification

© ECMWF, 2002

of a_P, a_l, D, and the subgrid scale assumptions involved in P^*.

a_P, expressing the probability of interception of rainfall by the canopy, is estimated to be 0.75 over a Corsican pine plantation, by Rutter *et al.* (1972), while Shuttleworth (1988a) gives 0.92 for the Amazon forest. Warrilow *et al.* (1986) and Dolman and Gregory (1992) use $a_P = 1$. The sensitivity of daily canopy evaporation to the value of a_P is small when a_P lies between 0.85 and 1 (Shuttleworth, 1988b). Noilhan and Planton (1989) set $a_P = C_v$, where C_v is the fraction of the grid box covered by vegetation, while Blondin (1991), somewhat empirically uses $a_P = 0.25C_v$, probably as an attempt to include the subgrid-scale variability of interception.

When an interception model is used to validate point measurements, the observed precipitation rate can be used directly as a forcing term in Eq. (25), $P^* = P$. However, global model grid boxes vary between 60×60 km^2 and 400×400 km^2 and, for this scales, it is unrealistic to assume an uniform coverage of precipitation over the grid box, particularly in the case of convective precipitation. The atmospheric parametrization schemes provide an average rainfall rate representing the average value over the grid box, separated in large-scale precipitation (occurring due to supersaturation of the mean values of humidity) and convective precipitation. The subgrid distribution of precipitation is described in many hydrological and meteorological papers. A review of formulations that have been applied to GCMs can be found in Thomas and Henderson-Sellers (1991) and Pitman *et al.* (1993); see also Chapter 4 for an example of the sensitivity of the surface branch of the hydrological cycle of GCMs to the subgrid scale distribution of precipitation. A proper way of taking into account the heterogeneity should be dependent on the grid box size and the time step used. Note that although the instantaneous cover of precipitating convective elements within a grid box is a small value (of the order of 0.1), the effective cover can be several times larger, in order to take implicitly into account the movement of convective cells inside the grid box during one time step. Two distributions for precipitation intensity inside a grid box have been used: an exponential distribution (Shuttleworth, 1988b), and a box distribution (Viterbo and Illari, 1994). The idea is to assume that an equation like (25) holds for each grid point, with $P^* = P_l$ where P_l represents the local precipitation rate: the value of P^* is obtained by multiplying P_l by its probability density function (pdf) value and integrating over the grid box. Note that P, the grid-box precipitation rate given by the atmospheric forcing, is the expected value of P_l over the grid box. P^* obtained in this way depends on a shape parameter of the pdf which, for the box distribution of Viterbo and Illari (1994), is the fraction k of the grid box covered by precipitation, taken as 1 for large-scale precipitation and 0.5 for convective precipitation. For the functional form of P^* using the exponential distribution see Dolman and Gregory (1992); a slightly different distribution was used by Eltahir and Bras (1993).

Let us now turn our attention to the evaporation part of Eq. (25). The fraction a_l multiplying the potential evaporation rate was first defined by Rutter *et al.* (1972) as W_l/W_{lmx} where W_{mx} is a constant, the maximum capacity of the interception reservoir. Assuming a constant potential evaporation, Eq. (25) will give an exponential decrease of the water in the interception reservoir. Under the sole effect of evaporation the interception reservoir would never go to zero, which led Deardorff (1978) to assume a power law for $a_l = \min[1, (W_l/W_{lmx})^{2/3}]$. The previous expression can be multiplied by the vegetation cover, in which case $(W_l/W_{lmx})^{2/3}$ can be interpreted as the fraction of the vegetation cover that is wet (Warrilow *et al.*, 1986, Noilhan and Planton, 1989). The maximum size of the interception reservoir, W_{lmx}, is proportional to the leaf area index, L_f times the amount of water that can be stored on a single leaf (W_{max}) or, in case the reservoir includes ponding of bare soil (Blondin, 1991),

$$W_{lmx} = [C_v L_f + (1 - C_v)] W_{max} \tag{26}$$

The remaining term to be specified in Eq. (25) is drainage. This is the term where most existing formulations differ. We will disregard stem flow in our discussion, because its consideration require an additional reservoir of water related to the storage in the trunks (Rutter *et al.*, 1975). Formulations in the literature are divided in two broad classes: i) Allowing drainage before the interception reservoir is saturated (Rutter *et al.*,1972, Warrilow *et al.*, 1986, or Dolman and Gregory, 1992, for the case of a subgrid scale distribution of precipitation); ii) Threshold for-

© *ECMWF, 2002*

mulations, where drainage occurs only if the reservoir is saturated (Dickinson, 1984, Noilhan and Planton, 1989, or Blondin, 1991, for the case of subgrid scale distribution of precipitation).

The total storage of the canopy reservoir, W_{lmx}, is the main parameter controlling the behaviour of a particular interception model (Shuttleworth, 1988b). Model results are also sensitive to details of the subgrid distribution of precipitation, as shown by Shuttleworth (1988b), Dolman and Gregory (1992), Thomas and Henderson-Sellers (1991) and Viterbo and Illari (1994). If the canopy storage is also allowed to vary within a grid box, the drainage and interception terms assume a different form, depending on the assumed pdf distribution for W_1: a complete generalization of Eq. (25) can be found in Eltahir and Bras (1993).

Since the processes described in this section are very fast (small timescales), the integration of Eq. (25) poses some numerical problems. The first is stability: the method of Kalnay and Kanamitsu (1988) is commonly used, where the fastest non-linear term (evaporation) is treated implicitly. The second problem relates to time truncation errors (see Dolman and Gregory, 1992). The third problem is mass-conservation: it is not trivial to formulate a numerical implementation of threshold methods for the drainage term that conserves mass for the watersubstance. In the ECMWF model, a rate of evaporation from the interception reservoir is needed for the specification of the total evaporation, for use as a boundary condition for the turbulent vertical diffusion of water vapour in the atmosphere. Because of the semi-implicit scheme used in the time integration of the surface equations, it is not possible to ensure a perfect matching between wet evaporation, as seen by the atmosphere, and the amount of water lost by the interception reservoir. Viterbo and Beljaars (1995) discuss a scheme that attempts to minimize the different time truncation errors described above, while at the same conserving the mass of the water substance and having the necessary requirements of stability.

3.3 (d) Runoff and infiltration. A proper account of runoff is not common in most GCMs, especially those used in NWP. In connection with ongoing international programs, such as the Global Energy and Water budget EXperiment (GEWEX) and the GEWEX Continental-scale International Project (GCIP), it is likely that this situation will change rapidly in the near future. Note that a correct treatment of runoff will be specially important for coupled ocean–atmospheric models (to define the fresh-water inflow to the oceans) and long timescales. In this section, some basic terminology and concepts from hydrology will be introduced and the relation with similarly named quantities in GCMs will be explored. A qualitative description of runoff will be presented, emphasizing its role in the soil-water controlled part of the hydrological rosette (phases A–D, Fig. 3). A rainfall-runoff scheme, making use of subgrid-scale distribution of soil parameters, and currently used in GCMs (Dümenil and Todini 1992; Liang *et al*. 1994) is presented; all other discussions related with subgrid heterogeneity are postponed to Section 5. Two routeing schemes, for the lateral transport of soil water in GCMs, are referred to. They allow the computation of fresh water discharge of the major rivers into the ocean, and can be used directly during a coupled ocean-atmosphere GCM run, or for post-processing the GCM output. The model runoff averaged over a large basin is often compared to river discharge to the oceans (see e.g. Dümenil and Todini 1992)

Infiltration is that part of the precipitation flux that contributes to wet the soil. At the interface soil–atmosphere, the continuity of the water flux can be written as

$$I_{\mathrm{f}} = T - Y_{\mathrm{s}} \tag{27}$$

where I_{f} and Y_{s} are, respectively, the infiltration and the surface runoff (units kg $\mathrm{m}^{-2}\mathrm{s}^{-1}$). Eq. (27) is part of the boundary condition to integrate Eq. (15) for the soil water transfer, the remaining part being evaporation. For most GCMs, and certainly for all current NWP models, Eq. (27) defines Y_{s} as a quantity that is lost to the model water cycle; there is no horizontal transfer of water in the soil. Y_{s} represents in these GCMs an instantaneous, local response to precipitation, with no time-lag and no notion of a drainage network or a drainage basin attached to it. Y_{s} is a scalar because no direction of water transfer needs to be specified.

© ECMWF, 2002

In hydrology studies, Y_s in Eq. (27) represents a divergence of an horizontal soil-water flux at the surface. The possible different paths taken by the rainfall and snow-melt water, until it reaches a stream channel, are described schematically in Fig. 6 (from Dunne 1978). Water impinging on a hillside of limited infiltration capacity becomes *overland flow*, but if the precipitation (snow melt) is absorbed by the soil and encounters some shallow depth of impervious material, it creates a subsurface horizontal flow, named *subsurface streamflow.*

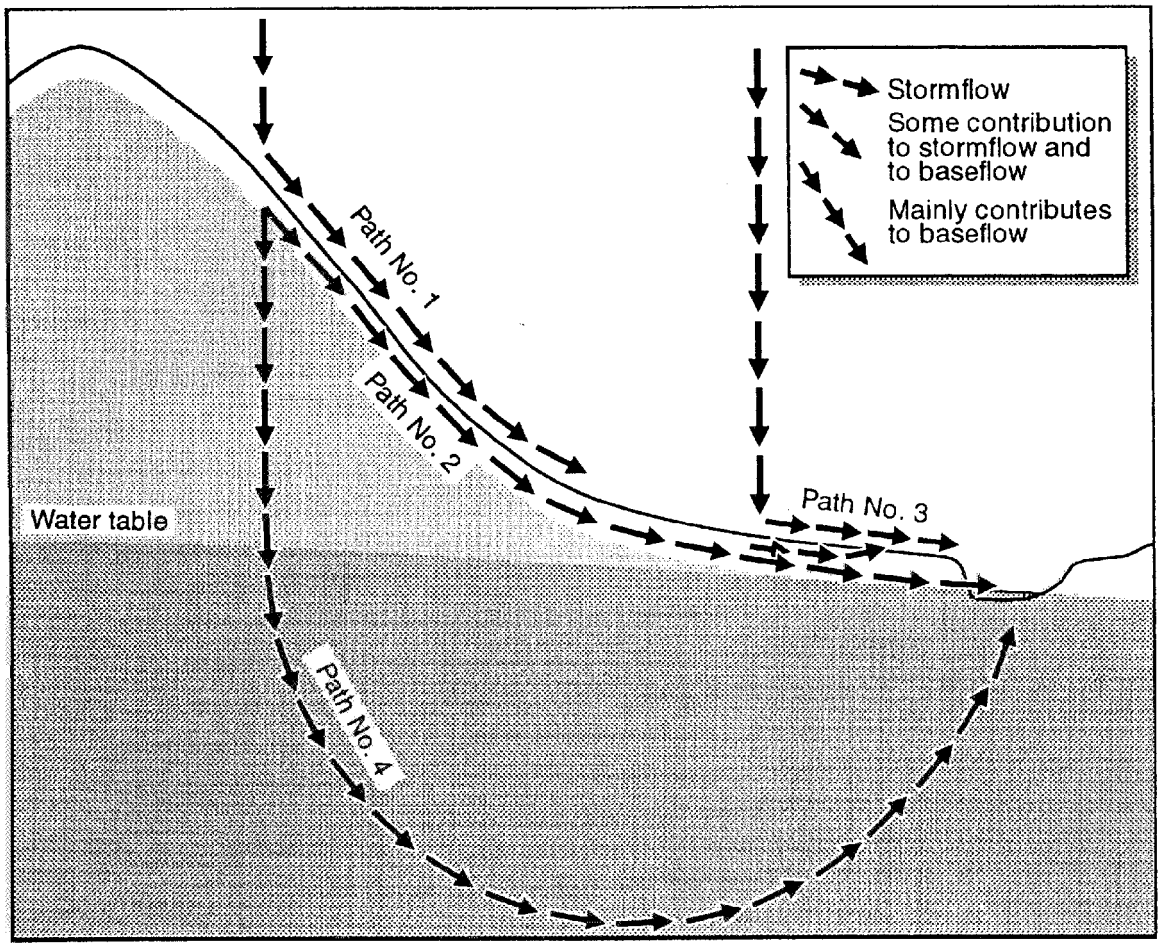

Figure 6. Possible flow paths of water moving downhill (from Dunne, 1978).

Subsurface streamflow that returns to the ground surface and leaves the hillside is named return flow; together with the precipitation that falls into saturated areas, they form the *saturation overland flow.* Finally, if precipitation is absorbed by the soil it will slowly percolate until it reaches the saturated zone in the soil, and will eventually be diverted horizontally to the nearest stream channel. The water collected by the different paths detailed above, arrives to the stream channels and is collected in catchments of different sizes until eventually arriving at the ocean as fresh-water inflow.

The role of parametrization in GCMs, with regard to the term Y_s, would be to represent the transport by the above four mechanisms, plus the water transport by the stream channels. The timescales of the response to a precipitation event by each of the above mechanism are very different. Hydrologists separate flow into a *streamflow* responding directly (but with a time and space lag) to a precipitation event, and a *baseflow* that is the part of the flow that is, to a large extent, independent of precipitation events (but its intensity will reflect long-term anomalies of precipita-

© ECMWF, 2002

tion). The first three mechanisms described in Fig. 6 are essentially contributors to storm runoff, while path 4 will be a contributor, partly to the baseflow and partly to the storm flow (depending on the position of the water table).

As described in Fig. 3 , when precipitation starts, following a dry spell, it will first meet a dry soil with a large infiltration capacity (route B–C in the figure); the rate of change of soil wetness is determined by the precipitation rate, the regime is atmospheric controlled. If the precipitation event is long enough, the infiltration capacity—the maximum rate of top infiltration for a given soil condition—will reduce while the soil gradually fills up with water, until it eventually becomes smaller than the precipitation rate (point D in the picture). Beyond that point, part of the precipitating water goes into runoff; the fraction of water that goes into runoff is determined by the soil state and its morphology, area C–D in Fig. 3 is under soil control.

Two possible mechanisms, namely the Horton runoff and the Dunne runoff (see, e.g. Bras 1990), have been identified to describe the different water paths in Fig. 6 . Any real runoff event will be due to either one of the two mechanisms or to a combination of the two, depending on the precipitation intensity, the type and state of the soil, the morphology of the terrain, and the soil cover. The Horton mechanism occurs mainly in upslope areas, in those parts of the watershed where conductivities are lowest; runoff occurs in areas where the infiltration capacity is lower than the precipitation rate. The near-surface soil-water content increases until the hydraulic conductivity at the surface (or infiltration capacity) is identical to the precipitation rate; beyond that point runoff occurs. The soil wetting front comes from above in this mechanism. In the Dunne mechanism, in near-channel wetlands, the overland flow or surface runoff will occur when the water table rises up to the surface; it happens preferentially in those parts of the watershed where the water table is shallowest. Runoff starts when the water table rises and eventually meets the surface; the soil wetting front comes from below in this mechanism. The Horton mechanism was the first to be identified, and is responsible for runoff in arid and semi-arid areas, where the total annual precipitation will tend to come in only a few large events, or in humid areas where the original vegetation and soil structure has been destroyed; the reduced vegetation cover or soil erosion creates a land surface with low infiltration capacity. In humid temperate areas with a dense vegetation, the soil infiltration capacities are larger and the precipitation is well distributed during the year; the Dunne mechanism will be predominant.

It is clear from the above description that the runoff fraction (Y_s/P) will depend on the soil type, terrain slope, moisture conditions, vegetation cover, precipitation intensity, and subgrid-scale variability of the above.

The Arno scheme, designed to represent in a GCM some of the basic mechanisms detailed above, is presented in the following. Based on a standard hydrological ‘lumped’ model (Becker 1992), it was adapted for use in GCMs by Dümenil and Todini (1992) and Wood *et al*. (1992), in connection with a single soil-moisture reservoir (‘bucket’), and later with multi-level reservoirs (Liang *et al*. 1994; Katia Laval, personal communication). The version of Dümenil and Todini (DT) is described. The original bucket model, without the ‘hydrology’ parametrization gives the time variation of water in a soil of depth D

$$\rho_w D \frac{\partial \theta}{\partial t} = P - Y_s + E \tag{28}$$

where $P - Y_s = I_f$ and I_f is computed as a threshold quantity

$$\begin{aligned} I_f &= P \qquad D\theta < W_c \\ I_f &= 0 \qquad D\theta \geq W_c \end{aligned} \tag{29}$$

W_c is the capacity of the reservoir, originally defined as 15 cm worldwide by Manabe (1969). The term Y_s has been generalized by DT to represent storm runoff as overland flow and drainage through the reservoir. To compute the storm runoff, a local balance equation of precipitation, runoff and infiltration (similar to Eq. (29)), is coupled

© ECMWF, 2002

to a subgrid-scale distribution of local storage capacity. For a given water content, w, the storage capacity distribution is the fraction of the basin area (or grid-cell in a GCM) for which the infiltration is less or equal w. Using that information for the spatial distribution of water, the local balance equation can be integrated for the entire basin. The shape of the storage-capacity distribution curve can be parametrically controlled, dependent on the standard deviation of orography in a grid cell; steeper subgrid-scale slopes imply larger values for runoff. A grid value for storm runoff, taking into account the subgrid-scale distribution of soil moisture, is therefore obtained.

Runoff, as produced by Eq. (29), together with the model subgrid-scale distribution assumptions, represents the amount of water that is lost locally by the system soil–atmosphere; we will refer to Y_s in this section as the source runoff (Miller *et al*. 1994). A horizontal advection scheme in the soil can be applied to that field of local imbalance, or source runoff, to produce an horizontal flow of water across land grid boxes, eventually arriving into the mouth of the rivers. If M (units kg m^{-2}) represents the water in the soil that is free to move (representing the river flow and groundwater flow),

$$\frac{\partial M}{\partial t} = \nabla \cdot \boldsymbol{F} + Y_s \tag{30}$$

where $\boldsymbol{F}$ (units kg m^{-1}s^{-1}) is a vector field representing the horizontal flux of water in the soil/surface of the model. It is proportional to the quantity of water upstream, with the direction and the proportionality being a specified set of advection rates u. Sausen *et al*. (1994) and Miller *et al*. (1994) present alternative ways of defining the advection rates.

4. EXAMPLES OF PARAMETRIZATION SCHEMES

As emphasised in the previous sections, land-surface parametrization schemes for use in GCMs define the surface boundary conditions for the atmospheric momentum, heat and moisture equations; surface stress, surface sensible-heat flux and surface evaporation flux, respectively. Because of the long timescales involved with soil moisture, and because of the diurnal cycle of the forcing (the net radiation at the surface), the land-surface parametrization schemes need to deal accurately with a timescales ranging from 1 hour to several months

The Project of Intercomparison of Land-Surface Parametrization Schemes (PILPS, Henderson-Sellers *et al*. 1993) is at the centre of a very large project coordinating the modellers' efforts. Its goals include a review of existing parametrization schemes (part of Phase I, has already been completed), followed by comparison of the model results when forced by synthetic data sets and field experiment data. Table 1, from Pitman *et al*. (1993) summarises the characteristics of a large number of schemes. Many schemes include a fast-responsive reservoir for evaporation (the interception reservoir), and separate descriptions of evaporation from the bare ground and transpiration. The representation of longer timescales (such as a complete cycle of the hydrology "rosette" in Fig. 3) is guaranteed if the soil water transfer is capable of quick infiltration of soil water at the beginning of a precipitation event, and retention of that water in the soil until the evaporative demand of the atmosphere reclaims it. Heat stored in the soil during summer can serve as a source of energy for the winter months. Finally, in high latitudes or over mountains, the representation of the insulation effects of the snow mantle, with its higher albedo and large heat capacity, is essential for a bias-free near surface temperature.

© ECMWF, 2002

TABLE 1. CHARACTERISTICS OF SEVERAL LAND-SURFACE PARAMETRIZATION SCHEMES

Key model	Number of canopy layers	Interception treated	Number of layers included for			Canopy	Philosophy for temperature	Soil moisture	Reference
			T	θ	Roots				
A. BATS1E	1	Yes	2	3	2	Penman/Monteith	Force-restore	Darcy's law	Dickinson *et al.* (1986,1993)
B. BEST	1	Yes	3	2	2	Penman/Monteith	Force-restore	Philip de Vries	Pitman *et al.* (1991) Cogley *et al.* (1990)
C. BUCKET	0	No	0	1	1		Instantaneous surface heat balance	Bucket + variation	Robock *et al.* (1993)
D. CLASS	1	Yes	3	3	3	Penman/Monteith	Heat diffusion	Darcy's law	Verseghy (1991) Verseghy *et al.* (1993)
E. CSIRO	1	Yes	3	2	1	Aerodynamic	Heat diffusion	Force-restore	Kowalczyk *et al.* (1991)
F. GISS	1	Yes	6	6	6	Aerodynamic	Aerodynamic	Darcy's law	Abramopoulos *et al.* (1988)
G. ISBA	1	Yes	2-3	2	1	Aerodynamic	Force-restore	Force-restore	Noilhan and Planton (1989)
H. TOPLATS	1	Yes	1	2	1	Penman/Monteith	Heat diffusion	Philip de Vries	Famiglietti and Wood (1994)
I. LEAF	1	Yes	7	7	3	Penman/Monteith	Heat diffusion	Darcy's law	Avissar and Pielke (1989)
J. LSX	2	Yes	6	6	6	Penman/Monteith	Heat diffusion	Philip de Vries	
K. MAN69	0	No	1	1	1			Bucket	Manabe (1969)
L. MILLY	0	No	1	1	1			Bucket	Manabe (1969)
M. MIT	0	No	3	3	3		Heat diffusion	Darcy's law	Abramopoulos *et al.*(1988) Entekhabi and Eagleson (1989)
N. MOSAIC	1	Yes	2	3	2	Penman/Monteith		Darcy's law	Koster and Suarez (1992)
O. NMC-MRF	1	Yes	1	1	1	Lumped with soil			Pan (1990)
P. CAPS	1	Yes	2	2	1	Penman/Monteith	Heat diffusion	Diffusion	Mahrt and Pan (1984)
Q. PLACE	1	Yes	30	30	2	Ohm's law analogy	Force-restore	Force-restore	Wetzel and Chang (1988)
R. RSTOM		No	0	1	1			Bucket + variation	Milly (1992)
S. SECHIBA	1	Yes	2	2	1	Penman/Monteith	Force-restore	Choisnel	Ducoudré *et al.* (1993)
T. SSIB	1	Yes	2	3	1	Penman/Monteith	Force-restore	Diffusion	Xue *et al.* (1991)
U. UKMO	1	Yes	4	1	1	Penman/Monteith	Heat diffusion	Diffusion	Warrilow *et al.* (1986)
V. VIC	1	Yes	1	2	1	Penman/Monteith or full energy balance	Heat diffusion	Philip de Vries	Liang *et al.* (1994)

Land Surface Parametrization schemes (LSP) can be classified in two classes in terms of their potential use:

(i) For short, medium and extended range (1–2 days, 3–10 days, 10 days up to a season, respectively) forecasts with NWPs. Operational requirements and the sensitivity to critical conditions prohibits the use of too complex LSPs, with many prognostic variable parameters.

(ii) On the other hand, longer-term (climate) integrations are more dependent on initial conditions, and the complexity of advanced LSPs can be an advantage for correctly handling the atmosphere/ surface interaction.

Because of the lack of observations to initialise the surface state variables, land-surface models in the NWP context work very often in 'climate mode', with the initial conditions taken from a very-short-range forecast (see Section 7). Since this requires a correct handling of the longer timescales by the land-surface scheme, the trend should be to try to unify the schemes and abolish the above distinction (see Subsection 4.2) below, ISBA has been applied to both mesoscale and climate modelling).

In the following we describe a few schemes: the bucket model, chosen for its simplicity and historical importance; the ISBA model, a force–restore scheme; and the ECMWF model, a multi-level model of heat and soil-water transfer. The emphasis is on highlighting a few relevant properties; for a complete description of the features of each model the reader is referred to the documentation of these schemes.

4.1 The bucket model

The bucket model has been introduced by Manabe (1969) as the first attempt to parametrize land-surface processes in GCMs. It is based on Budyko's concept of evaporative fraction, β. The evaporation is the product of β times the potential evaporation. There is a single reservoir of water in the soil, with its contents changing with the com-

© ECMWF, 2002

bined action of precipitation and evaporation. β is given by the ratio of the current contents of the reservoir and its maximum capacity. Runoff exists when the reservoir exceeds its maximum capacity.

As mentioned in the previous section, the bucket model overestimates evaporation over bare ground in all regions, and over vegetated areas in dry conditions . Milly (1992) describes some improvements to the bucket model that greatly reduce the above bias. Delworth and Manabe (1988, 1989) demonstrated that, when coupled to a GCM, the bucket model correctly works as a low-pass filter to the precipitation forcing; it is capable, therefore, of correctly representing the soil as a source of low-frequency variability to the atmosphere via the evaporation. Pan (1990) has applied the single-reservoir concept, but uses a Penman–Monteith evaporation, estimating skin temperature under saturated soil conditions.

4.2 ISBA

ISBA (Noilhan and Planton, 1989) represents a refinement of the Deardorff (1978) model. The soil is composed of a thin reservoir at the top and the root layer underneath. The diurnal and seasonal timescale force the thermal equations while, for the water budget, the forcing for each layer is parametrized based on the soil texture and Clapp and Hornberger (1978) relationships. Evapotranspiration is a sum of the bare-ground component, the interception and the transpiration.

There are, however, several characteristics that distinguish ISBA. It is a model that has been applied successfully at single point (Noilhan and Planton, 1989), to the mesoscale and to global GCMs (Mahfouf *et al*, 1993). There has been a constant validation effort (see summarizing table in the paper by Mahfouf and Noilhan, 1994) comparing model results to observations in field experiments in a variety of atmospheric conditions and for a wide range of ecosystems. Moreover, the authors' demonstrate here that it is possible to derive the model parameters from soil/vegetation characteristics in a consistent way (Noilhan and Lacarrère, 1995); parameter definition is based on a thematic mapping of the terrain, and the concept of 'effective' parameters (see next section), representing the heterogeneity of the terrain in a GCM grid box.

4.3 ECMWF surface model

The motivation for developing the current ECMWF surface model (Viterbo and Beljaars, 1995), which has been in operations since August 1993, was to model correctly the heat and water air–soil transfer with timescales ranging from the daily cycle to the season. Diagnostics of errors of the previous model (Blondin, 1991), when compared against field experiments data (Betts *et al*., 1993, Beljaars and Betts, 1993) formed the basis for developing a new scheme. The new scheme has four predicted soil layers for water and temperature plus a predicted skin temperature, and a thin surface-water layer representing the interception of precipitation and the collection of dew. The bottom boundary conditions are zero heat flux and free drainage. The four soil layers have depths of 7, 21, 72, and 189 cm, with a root zone in the first three layers. The deepest layer acts as a reservoir and a memory for the longer timescales (of the order a year). The formulation of the soil hydraulic properties is based on the Richards equation with the Clapp and Hornberger (1978) relationships for the definition of the soil hydraulic diffusivity and conductivity.

The introduction of a skin temperature, which is calculated from flux equilibrium at an infinitesimally thin layer at the surface, reduces the errors in the ground heat flux and the phase errors in the sensible- and latent-heat fluxes at the surface. A smaller roughness length for heat (and moisture) than momentum was introduced with the following benefits: i) it increases the difference between the surface and air temperatures, verifying better with FIFE data (Betts and Beljaars, 1993); ii) it improves the accuracy of the surface longwave emission for the FIFE data (Beljaars and Betts, 1993); iii) it improves the simulation of winter evaporation for the Cabauw data set (Beljaars and Viterbo, 1994).

© ECMWF, 2002

The evaporation is based on a vegetation fraction, derived from the dataset of Wilson and Henderson-Sellers (1985), treating separately on a grid box the evaporation of the wet canopy fraction, the transpiration from the dry canopy, and the bare ground. The scheme has been extensively validated, with emphasis on the long timescales, based on single-column integrations for the FIFE, ARME and Cabauw data sets (Viterbo and Beljaars, 1995), and the SEBEX data set (Beljaars and Viterbo, 1995). Some examples of the one-column validation effort are presented in Section 6. Parallel with the one-column integrations, a five-year 3D run was performed (Viterbo and Beljaars, 1995), and the performance of the scheme in data assimilation/forecast mode was analysed for the US floods of July 1993 (Beljaars *et al*., 1995).

5. SUBGRID-SCALE HETEROGENEITY

The size of current GCM grid boxes ranges from 60×60 km (ECMWF T213 model used for NWP) up to $4° \times 5°$, while the time steps used range from 5 min up to 1 hour. It is clear that none of the variables or parameters described in the previous chapter are homogeneous in a GCM grid box. Specially for the larger time steps, the forcing applied to a surface scheme cannot realistically be assured to be uniform in time; e.g. convective precipitation hardly ever has a constant intensity during periods longer than 10 min. This section will describe ways of dealing with the heterogeneity in a grid box or subgrid-scale heterogeneity.

The land surface is heterogeneous in all spatial scales, both in its physiography and its physical state. For example, Wetzel and Chang (1987) report on an analysis of variance of soil moisture in the top 10 km of soil, for spatial scales ranging from 10^{-1} m^2 to 10^3 km^2, and they found significant variance in the whole spectrum. Another example of variability can be found in any satellite image of a snow covered surface, revealing heterogeneity in the snow cover, linked mainly (but not only) to terrain elevation and orientation of the slope.

The problems involved in subgrid scale heterogeneity can be illustrated with the water balance equation (15), together with the parametric relations for the conductivity and diffusivity (16), and the boundary conditions at the top, defining the surface water fluxes, and at the bottom, the drainage flux.

- The first non-homogeneous quantity is the evaporation flux. Parts of a grid box over land will be covered with vegetation which, in turn, can have moisture deposited on its leaves. In winter, there will be snow-covered and snow-free parts of the terrain. As detailed in the previous chapter, the rate of evaporation of all the above parcels will be substantially different. Heterogeneity in the fluxes (which are part of the output of a land-surface scheme) is discussed in Subsection 5.1.
- The main forcing term of Eq. (15) is precipitation. Precipitation is far from uniform in a grid box size portion of land: i) the size of the rain generating convective cells is typically 1/10 of a grid box (Emanuel *et al*, 1994); and ii) frontal rain shows very often organisation in the mesoscale, with variations in intensity in scales only partly resolved even in the finer resolution GCMs. Heterogeneity of the forcing is discussed in Subsection 5.2.
- Most of the components of the land-surface parametrization depend on parameters which cannot be considered homogeneous in a grid box, even in a uniform fractionof it: e.g. the dry-vegetation part of a grid box will have non-uniform evaporation rates arising from a varying canopy resistance, corresponding to different stomatal apertures within the canopy, due to a different phenological state. Other parameters (e.g. conductivities, diffusivities, roughness lengths) will vary in the same way. Heterogeneity of the parameters is detailed in Subsections 5.2–5.3.
- Finally, the variable soil moisture itself cannot be considered homogeneous in a grid box. Reasons include the variability in the forcings, the parameters and the fluxes, as described above, but also the non-accounted variability arising from, e.g. the differences in soil type, the terrain shape, the vicinity of local features like an aquifer or a shallow-water table, etc. 'Intrinsic' heterogeneity in the

© ECMWF, 2002

prognostic variable, e.g. that part of the variance that has not been taken into account by the above three items, is detailed in Subsection 5.4.

5.1 Heterogeneity in the surface cover

Let us consider a grid box with a fraction $(1 - C_{\mathrm{LSM}})$ covered by lakes. The land cover part of the grid box will have a fraction covered by snow, C_{Sn}. The snow free part will be covered by bare ground $(1 - C_{\mathrm{v}})$, while a fraction C_{l} of the vegetation will be covered by intercepted water. The grid-box evaporation can, therefore, be written as a weighted sum of the expression of each different section (Abramopoulos *et al*., 1988; Noilhan and Planton, 1989; Pitman, 1991; Blondin, 1991; Ducoudré *et al*., 1993):

$$E = C_{\mathrm{LSM}}\left[C_{\mathrm{Sn}}E_{\mathrm{Sn}} + (1 - C_{\mathrm{Sn}})\left\{ C_{\mathrm{v}}\{C_{\mathrm{l}}E_{\mathrm{l}} + (1 - C_{\mathrm{l}})E_{\mathrm{v}}\} + (1 - C_{\mathrm{v}})E_{\mathrm{g}} \right\}\right] + (1 - C_{\mathrm{LSM}})E_{\mathrm{SM}} \tag{31}$$

In the above expression C_{LSM} and C_{v} are constant, geographically prescribed fractions (although the vegetation cover C_{v} can be allowed to vary seasonally), while C_{Sn} and C_{l} depend on the nature of the surface and also on the state of the soil and, therefore, will vary in a forecast. Typically C_{Sn} will depend on the amount of snow and C_{l} on the water content of the interception reservoir. The lake evaporation, E_{SM}, the evaporation of intercepted water, E_{l}, and the snow sublimation, E_{Sn}, can be computed at the potential rate. Equation (19) can be used for dry canopy evaporation, E_{v}, while E_{g} can be computed by any of the methods discussed in Subsection 3.3 (b). Note that all the different evaporation rates will be computed in this approach by using a single value for the temperature and soil water, representative of the entire grid box.

If the different heterogeneity elements corresponding to its fraction are distributed randomly in a grid box, Eq. (1) gives a good approximation to the grid-box evaporation (type A heterogeneity, as detailed by Shuttleworth, 1988b). However, if there is organisation in the heterogeneity (e.g. a single rectangular lake occupying half a grid box) mesoscale calculations can develop and transport a significant part of the heat and water involved (Avissar and Chen, (1993) type B heterogeneity in the paper by Shuttleworth (1988b); see also Subsection 5.4).

The approach of Eq. (1) can be downscaled one step further. If there is more than one species present in the grid box, the transpiration can be written as (Ducoudré *et al*, 1993; Avissar and Pielke, 1989; Li and Avissar, 1994)

$$E_{\mathrm{v}} = \sum_{i=1}^{N_{\mathrm{v}}} C_{\mathrm{v}i}E_{\mathrm{v}i} \tag{32}$$

where the summation is done across the N_{v} vegetation species, with cover $C_{\mathrm{v}i}$. For the computation of $E_{\mathrm{v}i}$, a different canopy resistance function can be applied to each species. In this way, each grid box is schematically distributed in tiles (up to seven different vegetation ecotypes in Ducoudré *et al*, 1993). As for Eq. (31), Eq. (32) is only valid if the different micro-elements, which conceptually aggregated constitute a tile, are randomly distributed in the grid box. The approach detailed in Eqs. (31) and (32) is inexpensive, both in computational terms and in terms of memory. The only computational burden is to calculate the evaporation formula N times while carrying, in the case of Eq. (32), an additional file detailing the different ecosystems existing in a grid box.

One step further in the line of complexity is to have different energy and water budgets for each of the separate tiles (or fractions, as represented in the previous two equations). The grid box will be characterised not only by one temperature and soil water content, but N temperatures and N soil water contents, corresponding to the N different tiles (Avissar and Pielke, 1989; Li and Avissar, 1994). The cost in memory can be prohibitive for GCMs because it multiplies the number of surface prognostic fields by N. Note that all the different surface tiles will have

© *ECMWF, 2002*

the same atmospheric forcing, namely radiation, precipitation and near-surface atmospheric variables.

5.2 Prescribed subgrid-scale distribution of variables

Over a scale of 100 x 100 km, precipitation rate is far from uniform; the characteristic size of an individual convective element is of the order of 1–10 km, whereas its lifetime is of the order of the time step used in GCM models (0.5–1 hour). During that time the individual convective element will be advected, hence the fraction of the 100 x 100 km square wetted by the cloud will be larger than the value in any snapshot at any given time. The actual precipitation intensity will follow some distribution law, with slope and amplitude dependent on the grid rise and the time interval considered (Entekhabi and Eagleson, 1989; Warrilow *et al*, 1986). The output of a convection scheme in a GCM (e.g. Tiedtke, 1989) will be a precipitation rate corresponding to a mean rate in that time step and for the grid box considered. The partitioning of that rain into interception, and subsequently into infiltration and run-off, will be markedly different if the rain is assumed to fall uniformly or if, say, it falls in a fraction k of the grid box with amplitude P/k (see Viterbo and Illari (1994) for more details). The more concentrated in space the rainfall is, the higher are the chances of reaching soil infiltration limits and therefore of producing run-off.

Three distributions (probability density functions, pdf) of precipitation have been used in GCM modelling: a γ-distribution (Eagleson, 1978b; Entekhabi and Eagleson, 1989), an exponential distribution (Warrilow *et al*., 1986; Dolman and Gregory, 1992; Shuttleworth, 1988b; Pitman *et al*, 1990) and a box-distribution (Viterbo and Illari, 1994). All these distributions depend on parameters that define their sharpness; reliable estimation of these parameters based on observed events exists only for a handful of cases (e.g. Eagleson and Wang, 1985), with a larger uncertainty in the tropics because of the dearth of observational evidence. The sensitivity of the output of land-surface schemes (evaporation and run-off) to the value of the sharpness parameter was analysed: i) in stand-alone mode (i.e. running the land-surface model uncoupled from the GCM) by Pitman *et al* (1990) and Pitman *et al* (1993) (see also review by Thomas and Henderson-Sellers, (1991)) and ii) when fully coupled to a GCM (Viterbo and Illari, 1994). The sharpness parameter should be made dependent on resolution (Eltahir and Bras, 1993); it depends on the grid rise Δx, the time step Δt and the precipitation intensity P.

When a (pdf) $g(P_i)$ for precipitation exists, the fraction of the grid box with rainfall intensity between P_i and $P_i + \mathrm{d}P_i$ is $g(P_i)\mathrm{d}P_i$, with $\int_0^\infty g(P_i)\mathrm{d}P_i = P$. Applying Eq. (15) for the soil-water balance over that fraction of the grid box, the forcing is written as $g(P_i)\mathrm{d}P_i$, and the result can be integrated across the range of precipitation intensities. The scheme integration can be made numerically (with techniques similar to the ones detailed in Avissar and Pielke (1989)) during the GCM integration, or analytically beforehand (Dolman and Gregory, 1992). The latter case will produce a modified Eq. (15); for simple distributions the modification made to the equations is trivial (Viterbo and Illari, 1994).

The technique detailed above can be applied to any variable; a statistical–dynamical approach for considering heterogeneity is any approach where the variations in the input and the model state are quantified in terms of different probability density functions (pdfs), and the output computed as the contribution of the forcing with the different model states, properly weighted by their own pdf functions. The run-off scheme of Dümenil and Todini (1992) presented in Subsection 3.3 is another example where the infiltration capacity of the soil in a grid box is assumed to follow a distribution law. Further examples can be found for variations one parameter (Avissar, 1992) or in the state variables (Wetzel and Chang, 1988; Johnson *et al*, 1993). Avissar (1992) considers the subgrid-scale variation of stomatal conductance. The surface energy-budget equation is written for a given value of stomatal conductance. The appropriate soil-water and heat equations are also computed for the given value of stomatal conductance. The system is valued for the ground surface temperature. The result is computed numerically for all values in the range of stomatal conductances and the solutions are averaged according to the pdf. Wetzel and Chang (1988) consider their statistical–dynamical variations of both the soil water (with a pdf taken from observations) and of stomatal resistance. Averaged results are computed numerically by double integration across the soil-moisture and

© ECMWF, 2002

the stomatal-resistance ranges, and the results are compared with observations. The traditional approach, considering only mean grid-square values, is shown to underestimate evaporation in cases of dry soil and underestimates it when the soil is close to field capacity. Johnson *et al* (1993) report on the testing within a GCM of a scheme where both run-off and evaporation used pdfs to characterise their dependence on precipitation and soil wetness. Their method generalises Dümenil and Todini's (1992) work. Finally, Mahrt (1987) computed the grid-averaged surface fluxes when the static stability is not uniform in one grid box.

5.3 Effective parameters and blending height

As mentioned before, the effect of subgrid-scale heterogeneities depends on their length scale. For smaller length scales (less than 10 km) no organization is seen in the PBL and turbulence is responsible for the vertical transport of heat, moisture and momentum (Shuttleworth, 1988b). For the above conditions it is possible to define the *blending height*, the minimum height in the PBL where mean atmospheric conditions are approximately in equilibrium with the underlying surface (Wieringa, 1986; Mason, 1988; Claussen, 1991). As an example, let us consider the dry vegetated part of the canopy, fraction $C_v(1 - C_l)$ in Eq. (31). Previously, we have already seen how to compute the average surface flux as a mean across the heterogeneity elements of terms proportional to the difference between an atmospheric term and the appropriate surface term. The atmospheric term has to be computed at (or above) the so-called blending height.

A simpler alternative way of considering the heterogeneity in, e.g., the dry vegetated part of the canopy, is to use values of a mean surface state in the computation of the fluxes, but with modified parameters in the transfer coefficients (or surface resistances). The modified parameters that yield the correct value for the mean fluxes are called *effective parameters* (Fiedler and Panofsky, 1972; Mason, 1988; Warrilow and Buckley, 1989; Noilhan and Lacarrère, 1995). It is useful at this stage to distinguish between *primary* parameters and *secondary* parameters (Noilhan and Planton, 1989; Noilhan and Lacarrère, 1995). In the following, we assume that a dataset of the primary parameters exists at a finer resolution than the GCM resolution. The values of a few primary parameters (e.g. depth of soil, dominant type of soil texture, dominant type of vegetation) in a detailed dataset determine the values of secondary parameters (roughness length, LAI, main stomatal resistance, fractional vegetation cover) at the resolution of the original data set. The problem consists of finding an effective value of each of the secondary parameters at the GCM resolution by stable averaging procedures. The averaging operator for each parameter is chosen for consistency with an arithmetic averaging of the fluxes themselves; in other words, for a given parameter, the average should be linear in the related quantity that scales linearly with the fluxes. For instance the effective canopy conductance of a GCM grid box is defined as a weighted sum of the conductances of the elementary areas (for other examples see Warrilow and Buckley (1989) and Noilhan and Lacarrère (1995)).

© *ECMWF, 2002*

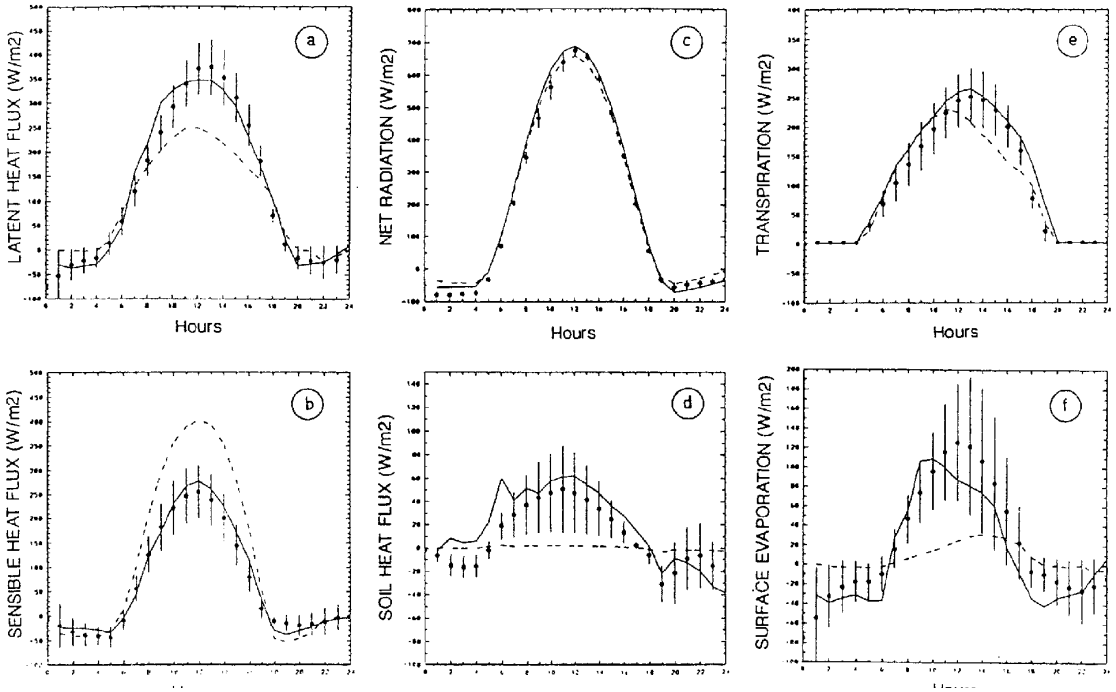

Figure 7. Comparison between the area-averaged surface fluxes computed from the 3D model (solid points) and the 1D prediction with dominant (dashed line) or effective (solid line) properties. The vertical bars represent the standard deviation of the fluxes in the 3D model. (a) Latent heat flux, (b) sensible heat flux, (c) net radiation, (d) soil heat flux, (e) plant transpiration, and (f) bare soil evaporation (from Noilhan and Lacarrère, 1995).

Fig. 7 presents a comparison between the fluxes computed with a detailed mesoscale model and the fluxes computed using the effective parameter concept for a situation in the HAPEX–MOBILHY database (André *et al.*, 1986). Despite the nonlinearity of the dependence of surface fluxes on vegetation parameters and soil-water content, it is clear that the effective surface fluxes computed with a 1D model match the 3D mesoscale estimates with a relative error of ±1.0 %. For the cases examined, the effects of nonlinearity were found to be smaller for the vegetation parameters (e.g. stomatal conductance) than for the soil-water transfer parameters (e.g. hydraulic diffusivity).

As pointed out by Noilhan and Lacarrère (1995) and Blyth *et al.* (1993), the effective parameter approach does *not* work when i) the mesoscale fluxes are of the same order of magnitude as the turbulent fluxes (see next section); and ii) the water, snow and ice surfaces are included in the average, because heat and evaporation fluxes are governed by quite different physical mechanisms. When one of those conditions exist, the fluxes should be aggregated using either Eq. (31), with a single surface temperature or different surface temperatures (Subsection 5.1).

5.4 Additional remarks

In the previous sections we have seen how variations in the input of the model and its parameters imply spatial variations in the output; the above variations would, in principle, be present at the smaller spatial scales (e.g. below 1 km) and hamper even the mesoscale simulations that are taken as 'truth' in most heterogeneity studies. Avissar (1991, 1992) calls variations in these spatial scales ' heterogeneity', and argues that some of the variability in these scales might be 'self-regulating' (Avissar, 1993). Studying the variations in stomatal resistance in an otherwise homogeneous potato field, he argues that a decrease in the stomatal resistance in a single leaf causes transpiration to increase and this, in turn, will humidify the surrounding air. As a result, the specific-humidity difference for a

© ECMWF, 2002

neighbouring leaf increases and causes the stomatal resistance of those neighbouring leaves to increase, thus compensating for the transpiration increase of the first leaf. If 'self-regulation' dominates, the sensitivity of quantities like stomatal resistance to environmental variables at the GCM scale is much less than its corresponding value at the plot scale.

For length scales of land-surface variations larger than 10 km, mesoscale circulations are generated that affect the whole depth of the PBL (Avissar and Pielke, 1989; Bougeault *et al*, 1991). The concept of blending height is no longer valid (Claussen, 1993). It has been argued that these circulations are responsible for the vertical transports of sensible and latent heat of the same order to magnitude as the turbulent fluxes (Li and Avissar, 1994; Chen and Avissar, 1994; Segal *et al*, 1988). Avissar and Chen (1993) present the equations for the so-called 'mesoscale kinetic energy', defined in a similar way to the turbulent kinetic energy (Stull, 1988) except that the averaging operator is limited to mesoscale lengths. The results obtained suggest mesoscale fluxes larger than turbulent fluxes are normally obtained in calm situations, whereas when there is some mean wind, turbulence takes over as the main mechanism of vertical transport. For the much more difficult problem of the vertical transport of heat and moisture in stable cases and in the presence of topography see the review by Kaimal and Finnigan (1994).

6. VALIDATION AND INTERCOMPARISON

6.1 Point validation

Results of field experiments measuring surface fluxes and variables as local point values, or on a regional scale, are regularly used to test surface parametrization schemes. To give just a few examples, ARME (Shuttleworth *et al*, 1984) data over the Amazon basin have been used in validating SiB (Sellers *et al*, 1989), ISBA (Noilhan *et al*, 1993) and the ECMWF new surface model (Viterbo and Beljaars, 1995). FIFE (Sellers *et al*, 1988, 1992) data over the Konza Prairie in Kansas, US and Cabauw data in the Netherlands have been used to validate the ECMWF model (Betts *et al*, 1993; Beljaars and Viterbo, 1994) and, in the case of FIFE, to validate ISBA. HAPEX/MOBILHY data in southern France have been used to test the ISBA model and the ECMWF model. SEBEX data, over the Sahelian region, have been used to validate the ECMWF model (Beljaars and Viterbo, 1995). For a review of recent experiments useful for the validation of surface parametrization data, the reader is referred to Shuttleworth (1991). Noilhan *et al*. (1993) describe all the validation efforts for what is probably the most thoroughly validated surface parametrization model, ISBA. A summary of field experiments is presented in Table 2. It is clear from that table that many valuable experimental datasets have never been used to validate any large-scale surface model. Snow is very much under-represented. Campaigns that have just finished for the Canadian boreal forest (BOREAS, Sellers *et al*, 1995) or are currently under way for the Scandinavian forest (NOPEX, 1994) will, hopefully, fill that gap in validation data.

© ECMWF, 2002

TABLE 2. RECENT FIELD EXPERIMENTS AND THEIR USE FOR VALIDATION OF LAND SURFACE MODELS.

Experiment	Reference	Location	Data	Model validation
ARME,1983–85	Shuttleworth *et al*. (1984)	Amazon basin	Surface energy and water balance, soil wetness	ISBA, SiB, ECMWF
SEBEX, 1989-90	Wallace *et al*. (1991) Dolman *et al*. (1993)	Sahel	As above	ECMWF
HAPEX–MOBILHY, 1986	André *et al*. (1986)	Southwest France	As above, information on mesoscale variability	ISBA, ECMWF, PILPS
Cabauw, 1987	Beljaars and Viterbo (1994)	Netherlands	Surface energy and water balance	ECMWF, PILPS
FIFE, 1987, 1989	Sellers *et al*. (1988, 1992)	Kansas, US	As above	ISBA, SiB, ECMWF
La Crau, 1987		Marseille, France	As above	
LOTREX, HIBE88, 1988		Germany	As above	
Niger, 1988		Northern Sahel	As above	
HEIFE, 1990		Tibetan plateau, Gobi desert	As above	
Kurex-88, 1987–88		Basin of river Seym	Hydrological data, including runoff and snow	
EFEDA, 1991-95		Central Spain	Surface energy and water balance	ISBA
HAPEX-SAHEL, 1992		Sahel	as above	
BOREAS, 1991–95		Canada	As above, snow measurements	
ABRACOS, 1991–95		Amazon basin	Surface energy and water balance	

In pointwise validation, the surface model runs coupled to a PBL model (1-column) or uncoupled (surface 1-column, or 0-column), are forced by time series of observed values. The quality of the model can be assessed by comparing its output (e.g. latent and sensible heat, or soil moisture time series) with observed values. 0-column validation requires a time series of observed values of surface wind and near-surface atmospheric temperature and humidity, solar radiation and downward long-wave reduction (Henderson-Sellers *et al*., 1993). The advantages are: i) current automatic measurement stations allow the measurement of the above quantities during several months, therefore the model behaviour can be validated in its longer timescales; ii) since radiation is part of the forcing, mismatches between the model output and observations can be attributed to the surface model's surface-flux formulation. On the other hand, because of the absence of negative feedback from the boundary layer, model drifts are perhaps exaggerated in this validation model (Jacobs and de Bruin, 1992). Nevertheless, 0-column validation remains the only form of validation giving a clear message about the quality of the land-surface scheme. A major intercomparison exercise, PILPS (Henderson-Sellers *et al*, 1993) is currently under way, whereby most of the existing surface models are compared in 0-column mode, forced first by synthetic datasets and then by a time series of observed values. The first observed data sets chosen were Cabauw and HAPEX/MOBILHY. It is planned, in the next phase of PILPS, to couple each of the land-surface schemes with the same host GCM and compare their behaviour in true interactive model. A similar European intercomparison exercise, SLAPS, was designed to assess the quality of the land-surface schemes when compared with catchment-scale models developed by hydrologists, and concentrates in the hydrological aspects of the land-surface schemes.

© ECMWF, 2002

When an estimate of the regional distribution of the fluxes is available (as in HAPEX/MOBILHY), another possible way of validation is to run a mesoscale model over the field-experiment area. This type of modelling has been essential in validating the equivalent-parameter concept (see previous section and Noilhan and Lacarrère (1995)) and is crucial for assessing the importance of the organisation of fluxes in the mesoscale (Avissar andPielke, 1989).

It needs to be stressed that the validation effort has be made in close cooperation between the experimentalists and the modellers, the former bringing their expertise in doing error analysis and suitable averaging of the data, while the latter bring the interpretation of model results and suggestions for improvement. Field experiments collect a very large volume of data (of the order of a few Gbytes, see Sellers *et al*. (1992)) that has to be aggregated into a much smaller set of values that will be the forcing data set for the surface model, and another set that will serve to validate the results (each set being no more than a few Kbytes). This is, by no means, a trivial exercise (Betts *et al*, 1993; Beljaars and Viterbo, 1995) but, once it has been done for use with one model, it is readily available for validating other models.

One final remark. Field experiments are normally organised with concentrated measuring efforts on a few days to few weeks, the so-called Intensive Observation Periods (IOPs), with gaps for some quantities, such as evaporation between two consecutive IOPs. Due to the different timescales involved in soil moisture (ranging from the diurnal to the seasonal scale), it would be desirable to have, in future experimental efforts, continuous monitoring of evaporation, radiation and sensible-heat fluxes, together with soil moisture in the root zone, at least for an entire season. In that way, a closed soil-water budget can be performed for the observations.

6.2 Other forms of validation

Forecast/assimilation systems have the infrastructure to monitor the forecast results against observations (Strauss and Lanzinger, 1993). Near-surface atmospheric variables routinely compared with the plentiful SYNOP observations include 2 m temperature and humidity, low-level cloudiness and precipitation. As detailed by Lanzinger (this volume), the interpretation of the data displayed gives important clues about model problems, and the signature of model/analysis changes is often found in a long time series of data.

A set of global-, continental- and regional-scale datasets that can be used to validate results from GCM climate runs or to monitor the performance of NWP assimilation/forecast systems is presented in Table 3. In this type of validation, it is not always obvious how to link errors in the variables to deficiencies in one specific parametrization scheme. For instance, feedbacks between model processes can be responsible for model deficiencies in a variable such as precipitation (Arpe, 1991). Some of the datasets in Table 3 are estimated; for instance latent-heat fluxes and the other components of the surface energy balance are estimated, based on the extent of empirical formulas and energy-conservation principles. These methods, although making the dataset self-consistent in energetic terms, cast some doubt on their validity for verifying model results.

To give another example, run-off data have been used to validate the model counterpart for major rivers (Russell and Miller, 1990; Dümenil and Todini, 1992). Most of the time problems in model run-off are related to deficiencies in model precipitation, rather than to the details of model surface drainage or infiltration. Separation of errors in forcing (the precipitation field) from the errors in the surface model is a difficult task (Miller *et al*., 1994).

© ECMWF, 2002

TABLE 3.GLOBAL DATA SETS THAT CAN BE USED TO VALIDATE SURFACE-RELATED GCM RESULTS.

Dataset	Parameter	(**M**easured/**E**stimated)/Area
Jaeger, 1983	Rainfall	**M** / global
Legates and Willmott, 1990	Rainfall	**M** / global
UNESCO, 1974	Runoff	**M** / global
Henning, 1989	Energy balance components	**E** / global
Wallis *et al*., 1991	Precipitation, runoff, temp.	**M** / US
Hollinger and Isard, 1994	Soil moisture	**M**/Illinois, US
Vinnikov and Yeserkepova, 1991	Soil moisture	**M** / former USSR
GCIP, 1995-2000	Water balance components	**M** and **E** / US

7. INITIAL VALUES

Despite the sensitivity of medium-range weather forecasts to the initial soil-water conditions (see reviews by Garratt (1993) and Rowntree, this volume), there are, at present, very few methods to define the soil-water content in data-assimilation systems. Current techniques for ground-based measurement of soil-water content (reviewed by Hillel (1982), Cuenca and Noilhan (1991) and Schulin *et al*. (1992)) include the gravimetric method, neutron scattering, electromagnetic techniques, and the tensiometer. None of these methods is adequate for routine measurements and, therefore, there has been an effort in recent years to provide satellite-based estimates of soil-water content (see reviews by Choudhury (1991) and Schmugge and Becker (1991)). The techniques can use information from the thermal infrared channels, or from active or passive microwave systems, but they have several calibration problems and provide only estimates for the water contents in the top few centimetres of the soil. We can safely state that *none of the current methods of measurement of soil water can provide a weekly global estimate of the soil-water contents in the root zone*.

Almost all schemes for initialisation of soil water in NWP are based on finding the equilibrium value of soil moisture, given *climatological* estimates of sensible- and latent-heat fluxes, and radiative fluxes at the surface (see e.g. Mintz and Serafini, 1992). They are, therefore, inappropriate for use with data-assimilation schemes, where the goal is to find a soil-water field representing an adequate balance of *real-time* estimates of the above fluxes. Many current NWP prediction systems circumvent the problem by assigning short-term forecast values to the initial conditions of soil moisture. Any deficiencies in the land-surface model or, more seriously, in the forcing terms (precipitation and net radiation) will cause the model to drift in time, and these short-term forecast values will eventually be affected by biases corresponding to the climatic bias of the land-surface model or the near-surface atmospheric forcing.

The only methodology that can be applied in a forecast/data-assimilation system is one based on the ideas of Mahfouf (1991). As mentioned in the previous section, the error of short-range forecasts of summertime near-surface temperature and dew point, when compared with the plentiful SYNOP observations (of the order of 10000 for any synoptic time), is normally a good indicator of the quality of the soil-water field; in broad terms, too warm and too dry near-surface atmospheric model states during daytime are associated with a wrong partitioning of the available surface radiative energy in latent- and sensible-heat flux, and with too dry values for the soil wetness. Mahfouf (1991) developed an optimal interpolation scheme for initialisation of soil water, relating the analysis increments of soil moisture to short-range forecast errors of near-surface temperature and dew point.

As with any data-assimilation scheme (Daley, 1991) used for medium-range forecasts, it is more important to initialise correctly the variables in the system associated with a longer memory, larger timescales. Variables with a subdiurnal timescale will adjust their initial values to some values compatible with the model physics; the adjustment process will take just a few hours, and beyond this adjustment period the ‘memory’ of the initial conditions

© *ECMWF, 2002*

is lost. For soil moisture, this means having a special concern about the deeper layers, other than the shallow top layer, because the former has a timescale of weeks, as compared with the diurnal timescale of the latter. Notice that the deeper layers still interact with the atmosphere via transpiration, transporting the water from the root layer to the atmosphere.

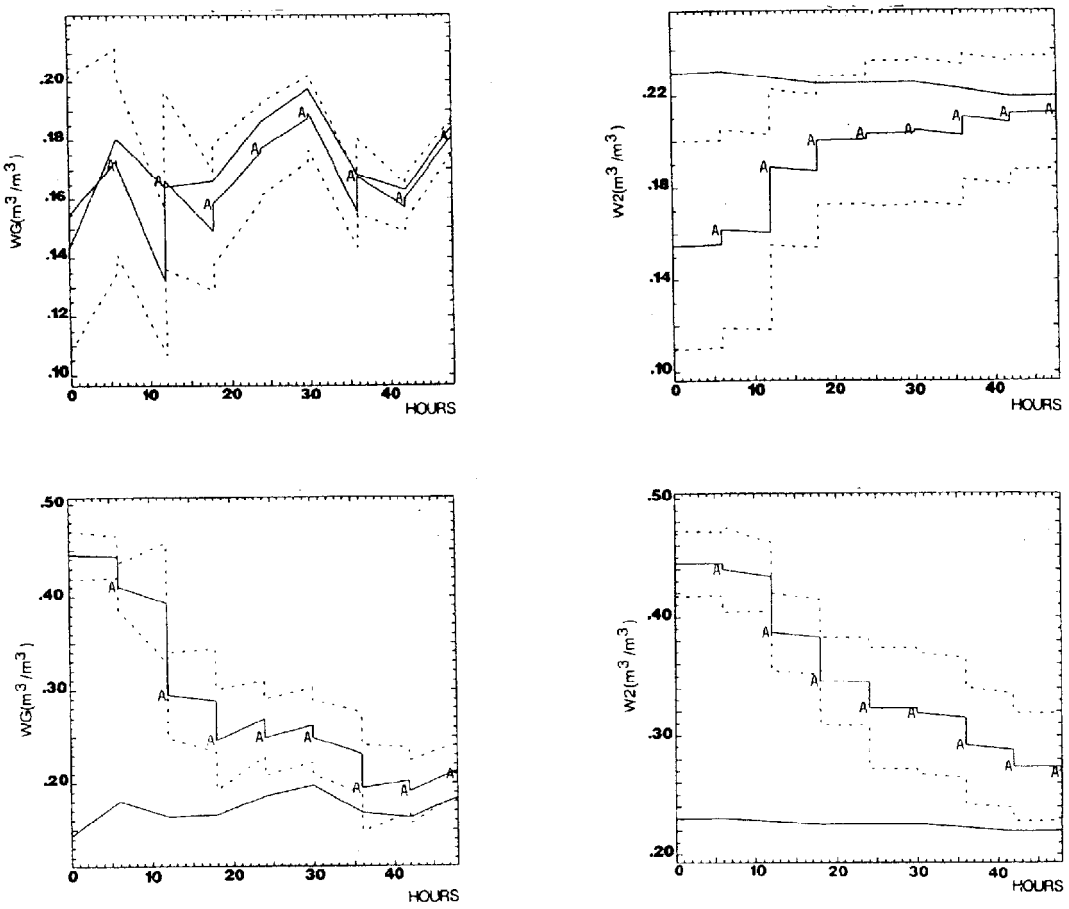

Figure 8. Evolution of soil water in 48-hour data assimilation with a mesoscale model. Top row: Starting condition dry. Bottom row: Starting condition wet. Values are shown for top soil water (left) and root soil water (right). Solid curves (A): mean values over the area; Dashed curves: maximum and minimum values; Solid curve, unlabelled: reference simulation, representing the truth (from Bouttier *et al*, 1993b)

Mahfouf (1991) developed an optimal interpolation scheme (Daley, 1991) for initialising the soil water, relating the analysis increments of soil moisture to short-range forecast errors of near-surface temperature and dewpoint. The scheme has been developed further and applied to the initialisation of soil water in a mesoscale model (Bouttier *et al*, 1993b). As shown by one-dimensional sensitivity and numerical simulation studies, in bare-ground areas the errors in the two-metre temperature and dewpoint are associated with errors in the *top* soil-water layer, while in vegetated areas it is related to the *root-layer* soil-moisture errors. The most critical aspect of the algorithm is the definition of the optimum coefficients in the matrix relating the errors in two-metre temperature and dewpoint to the analysis increment errors in the top and root-layer soil moisture. A continuous parametric formulation described in Bouttier *et al.* (1993a) allows for the computation of these coefficients at each model grid point. They will depend upon solar zenith angle and surface characteristics (vegetation coverage, roughness length and soil texture).

© *ECMWF, 2002*

A 48-hour clear-sky period from the HAPEX-MOBILHY experiment (André *et al.*, 1986) was studied by Bouttier *et al.* (1993b) and is presented in Fig. 8 . The results of the assimilation demonstrate the rapid convergence of the method when starting from a wet- or dry-soil moisture guess.

Recently, a simplified version of the Mahfouf (1991) algorithm was introduced into operations at ECMWF (Viterbo and Courtier, 1995). It corrects for a dry and warm bias in the surface and boundary-layer forecasts in late spring and early summer. The bias is associated to an underprediction of cloud cover causing too much solar radiation at the surface, driving too large an evaporation rate, and drying the soil too quickly and too early. The soil-water initialisation scheme prevents the soil-water values from drying too quickly. Fig. 9 , comparing the root-mean-square (rms) error for 20 forecasts run with (moist) and without (ops) the soil-water initialisation scheme, shows the large impact of the initial values scheme in the forecast quality. The impact on the rms comes mainly from a reduction in the lower-tropospheric bias of temperature; a wetter surface causes a colder lower troposphere and, due to the hydrostatic relationship, a shallower 20 kPa model surface. The large sensitivity of summertime continental forecasts to the definition of soil-water initial conditions confirms the results reviewed in Garratt (1993).

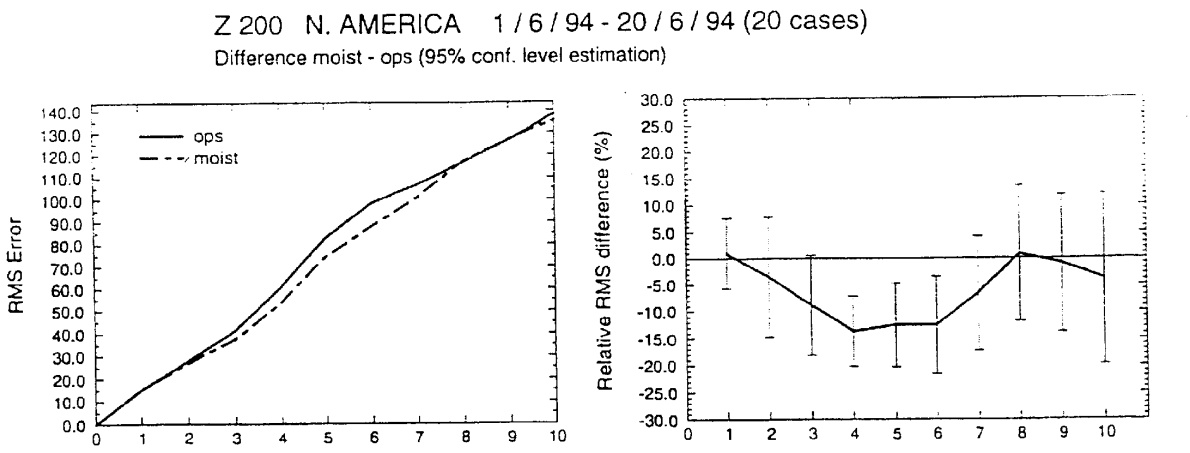

Figure 9. Mean root mean square of geopotential height for control (ops) and test (moist), and the mean difference and confidence interval at the 95% level, 1–20 June 1994, 20 kPa North America.

8. SNOW MODELLING

The effects of the snow mantle have to be taken into account for appropriate consideration of the surface thermal balance on high latitudes and mountainous regions in GCMs. The presence of snow reduces the energy available at the surface; the albedo of fresh snow is 0.85, while the albedo of a natural surface is in the range 0.12 to 0.25 (Dickinson, 1988). Snow melting is the most important source of soil moisture in spring in high latitudes. In general, due to its thermal properties, snow acts as an insulator between the air above and the soil underneath (Peixoto and Oort, 1992; Walsh *et al.*, 1985). The thermal and mass budgets of a layer of snow lying on the ground is relatively easy to establish on a local scale (e.g. Anderson, 1976), but more complex at scales of a typical GCM grid box, due to the heterogeneity of snow cover. In spite of its importance, there is very little observational evidence of relevance to GCMs on typical melting rates, albedo, snow cover and metamorphic changes followed by the snow mantle.

Most, if not all, current GCMs carry a prognostic equation for snow mass (Manabe, 1969)

© ECMWF, 2002

$$\rho \frac{\partial S}{\partial t} = F - M \tag{33}$$

where S is the snow depth (m of water equivalent), F is the snowfall (Kg $m^{-2}s^{-1}$) and M is the rate of melting. The snowfall is either given as an independent amount from other physical parametrizations in the model, or is the total amount of precipitation if the surface air temperature is below a certain threshold. The role of snow parametrization schemes is to specify the melting rate, M , and the snow albedo entering the thermal budget equation.

Melting conditions are met when the equilibrium ground temperature is above 0 C. In that case, an adjustment down to 0 C is made by melting the necessary amount of snow, while the upper soil reservoir collects the melted water. The melted water exceeding the maximum capacity of that reservoir is lost into runoff. Albedo in snow-covered areas is modelled as a background value plus a correction dependent on the snow amount. Some models take into account snow 'masking' by the vegetation in the computation of the albedo, so as to reduce the snow-covered area in the presence of tall vegetation, when compared with bare ground terrain (Blondin, 1991). The snow contribution to the albedo can also be made dependent on temperature; snow under melting conditions is made darker to simulate the effect of surface ponding (Dickinson *et al*., 1986).

Snow-cover fraction (the fraction of the grid box covered by snow) is important for its effects on the albedo and melting. Inspection of any satellite image reveals that snow-cover fraction is essentially dependent on vegetation, and on topographic details such as slope and aspect. In GCMs, the snow-cover fraction normally depends linearly on the amount of snow up to athreshold value, beyond which it is taken as 1. The threshold value can depend on roughness length, a crude way of parametrizing orography and vegetation effects.

More complex snow models are normally introduced by carrying extra predictive variables: snow density (Pitman *et al*, 1991; Verseghy, 1991; Douville *et al*, 1995), snow temperature (Verseghy, 1991; Dümenil, private communication),and snow albedo (Douville *et al*, 1995). Details of the snow-pack metamorphism, e.g. distinguishing between coarse and fine grain, or between old dark snow and finer fresh snow, can be considered by introducing a snow age (time elapsed since last snowfall, Verseghy, 1991) dependency on the density and on the albedo. For its independent thermal budget, the snow pack is considered as an additional variable-depth layer, with thermal conductivity and heat capacity dependent on snow density.

Melting of the snow pack can occur in these more complex models in two different ways: surface melting and deep melting. If the surface energy-balance equation gives a temperature above 0 C, melting of snow occurs at the expense of the excess of energy obtained by cooling the surface to 0 C. The resulting amount of water percolates into the snow layer and might refreeze within the snow pack at some unspecified depth, in a process called *ripening* of the snow pack. The remaining water wets the upper layer of soil. Deep melting occurs by heat conduction from underneath the snow pack if the soil is above 0 C. There is a adjustment of temperature, as in the surface melting, but no *ripening* is allowed, the water being immediately available to the soil layer. Note that a separate thermal budget of the snow layer is necessary for proper separation of the two melting mechanisms and the *ripening* of the snow pack.

As referred earlier in Section 3, phase change of the water in the soil is another important mechanism in high latitudes (Black and Tice, 1988, Williams and Smith, 1992, Miller, 1980). A parametric inclusion of the effects of the solid phase of water, although essential for modelling the soil water and energy transfer in high latitudes, is not considered in most GCM models. Its is possible to write additional equations for the conservation of frozen water at different soil layers (Verseghy, 1991, Pitman *et al*., 1991). Modifications to the traditional treatment include, in order of importance: i) The thermal effects related to the latent heat of fusion/freezing; ii) Substantial reduction in transpiration in the presence of a frozen ground; iii) Soil-water transfer dependent on a soil-water potential that includes the effect of frozen water. There are indications that these effects are very important for characterising the role of boreal forests in the climate system (Sellers *et al*., 1995).

© ECMWF, 2002

9. CONCLUSIONS

Current atmospheric models play a major role in estimating the surface branch of the hydrological cycle. The review presented above tried to emphasize the special role of NWP forecast/data assimilation systems as a continuously operating numerical laboratory for the study of the interactions of the atmosphere with the underlying surface. The only practical way of estimating globally the geographical distribution of the different terms of the surface hydrological budget on a day-to-day basis is to use data assimilation within a global forecasting system. In this systems, conventional synoptic data plus satellite observations are combined with a very-short-range forecast to produce an analysed state of the atmosphere. Short-range integrations starting from these initial states can provide an internally consistent (although model dependent) picture of precipitation, evaporation and runoff. Since the hydrologic formulation of current atmospheric models is a key component of the process described above, it is important to review the current state-of-the-art land-surface models, and to identify the deficiencies and areas where current research is likely to bring substantial improvements.

However, operational data assimilation systems do *not* provide a time-homogeneous sequence of values, because of the regular changes in either the data-assimilation methods or in the forecast model used. Alternative estimates, based on multi-year climate integrations of the model, are hampered by systematic errors in the models; they do not benefit from the corrective influence of the observations, regularly fed in the data-assimilation cycles. In order to combine the benefit of a long-period series of simulation given by the climate integrations with the controlling effect of the observations given by the data assimilation, several Centres started recently re-analysing the atmosphere with a frozen system (Bengtsson and Shukla, 1988). The ECMWF Re-Analysis Project is currently re-analysing the atmosphere at T106 31 levels, for the years 1979–1993. The project will be completed in 1996, and the examination of results related to the surface–atmosphere interaction will provide invaluable insight on mechanisms involved in different timescales, ranging from the diurnal cycle to the seasonal cycle.

The last 20 years have been characterised by a wide acceptance in the GCM community of the role of vegetation in controlling evaporation. The PILPS project is currently the catalyst in the only way ahead to develop and improve parametrizations: validation and comparison with observations. There is much to learn on the longer timescales of the atmosphere related to soil-water contents, the complicated interaction between soil water and precipitation, and the role of snow in the climate system.

REFERENCES

Abramopoulos, F., C. Rosenzweig, and B. Choudhury, 1988: Improved ground hydrology calculations for global climate models (GCMs): Soil water movement and evapotranspiration. *J. Climate*, **1**, 921-941.

Anderson, E.A., 1976: A point energy and mass balance model of a snow cover. NOAA Tech. Rep. NWS 19, 150 pp.

André, J.C., J.-P. Goutorbe, and A. Perrier, 1986: HAPEX-MOBILHY: A hydrologic atmospheric experiment for the study of water budget and evaporation flux at the climatic scale. *Bull. Amer. Meteor. Soc.*, **67**, 138-144.

Arpe, K., 1991: The hydrological cycle in the ECMWF short range forecasts. *Dyn. of Atmosph. and Oceans*, **16**, 33-59.

Avissar, R., 1991: A statistical-dynamical approach to parameterize subgrid-scale land-surface heterogeneity in climate models. *Land surface-atmosphere interactions for climate modeling. Observation, models and analysis.* E.F. Wood, Ed.,Kluwer, 155-178.

Avissar, R., 1992: Conceptual aspects of a statistical-dynamical approach to represent landscape subgrid-scale heterogeneities in atmospheric models. *J. Geophys. Res.*, **97D**, 2729-2742.

© *ECMWF, 2002*

Avissar, R., 1993: Observations of leaf stomatal conductance at the canopy scale: An atmospheric modeling perspective. *Bound. Lay. Meteor.*, **64**, 127-148.

Avissar, R., and F. Chen, 1993: Development and analysis of prognostic equations for mesoscale kinetic energy and mesoscale (subgrid scale) fluxes for large-scale atmospheric models. *J. Atmos. Sci.*, **50**, 3751-3774.

Avissar, R., and R.A. Pielke, 1989: A parametrization of heterogeneous land surfaces for atmospheric numerical models and its impact on regional meteorology. *Mon. Wea. Rev.*, **117**, 2113-2136.

Avissar, R., and M.M. Verstraete, 1990: The representation of continental surface processes in atmospheric models. *Rev. Geophys.*, **28**, 35-52.

Barton, I.J., 1979: A parametrization of the evaporation from non-saturated surfaces. *J. Appl. Meteor.*, **18**, 43-47.

Becker, A., 1992: Criteria for a hydrologically sound structuring of large scale land surface process models. *Advances in theoretical hydrology.* J.P.O'Kane, Ed.,Elsevier, 97-111.

Beljaars, A.C.M., 1995: The parameterization of surface fluxes in large-scale models under free convection. *Quart. J. Roy. Meteor. Soc.*, **121**, 225-270.

Beljaars, A.C.M., and A.K. Betts, 1993: Validation of the boundary layer representation in the ECMWF model. *Proc. Seminar ECMWF, 7-11 September 1992*, ECMWF, Reading, UK, 159-195.

Beljaars, A.C.M., and A.A.M. Holtslag, 1991: Flux parametrization over land surfaces for atmospheric models. *J. Appl. Meteor.*, **30**, 327-341.

Beljaars, A.C.M., and P. Viterbo, 1994: The sensitivity of winter evaporation to the formulation of aerodynamic resistance in the ECMWF model. *Bound. Lay. Meteor.*, **71**, 135-149.

Beljaars, A.C.M., and P. Viterbo, 1995: Soil moisture-precipitation interaction. In *Global energy and water cycles* (ed. by K. Browning and R. Gurney), to be published.

Beljaars, A.C.M., P. Viterbo, M. Miller, and A.K. Betts, 1995: The anomalous rainfall over the USA during July 1993: Sensitivity to land surface parametrization and soil moisture anomalies. Submitted to *Mon. Wea. Rev.*

Bengtsson, L., and J. Shukla, 1988: Integration of in situ and space observations to study global climate change. *Bull. Amer. Meteor. Soc.*, **69**, 1130-1143.

Betts, A.K., J.H. Ball, and A.C.M. Beljaars, 1993: Comparison between the land surface response of the ECMWF model and the FIFE-1987 data. *Quart. J. Roy. Meteor. Soc.*, **119**, 975-1001.

Betts, A.K., J.H. Ball, A.C.M. Beljaars, M.J. Miller, and P. Viterbo, 1995: The land-surface-atmosphere interaction. Submitted to *J. Geophys. Res.*.

Betts, A.K., and A.C.M. Beljaars, 1993: Estimation of effective roughness length for heat and momentum from FIFE data. *Atmos. Res.*, **30**, 251-261.

Black, P.B., and A.R. Tice, 1988: Comparison of soil freezing curve and soil water curve data forWindsor sandy loam. US Army Cold Regions Research and Engineering Laboratory, Hanover, New Hampshire, Report 88-16, 42 pp.

Blondin, C., 1991: Parametrization of land-surface processes in numerical weather prediction. *Land surface evaporation: Measurement and parametrization*, T.J. Schmugge and J.C. André, Eds., Springer, 31-54.

Blyth, E.M., A.J. Dolman, and N. Wood, 1993: Effective resistance to sensible- and latent-heat flux in heterogeneous terrain. *Quart. J. Roy. Meteor. Soc.*, **119**, 423-442.

Bougeault, P., 1991: Parametrization of land-surface processes for mesoscale atmospheric models. *Land surface*

© ECMWF, 2002

evaporation: Measurement and parametrization, T.J. Schmugge and J.C. André, Eds., Springer, 55-92.

Bougeault, P., B. Bret, P. Lacarrère, and J. Noilhan, 1991: An experiment with an advanced surface parametrization in a meso-beta-scale. Part II: The 16 June 1986 simulation. *Mon. Wea. Rev.*, **119**, 2374-2392.

Bouttier, F., J.-F. Mahfouf, and J. Noilhan, 1993a: Sequential assimilation of soil moisture from atmospheric low-level parameters. Part I: Sensitivity and calibration studies. *J. Appl. Meteor.*, **32**, 1335-1351.

Bouttier, F., J.-F. Mahfouf, and J. Noilhan, 1993b: Sequential assimilation of soil moisture from atmospheric low-level parameters. Part II: Implementation in a mesoscale model. *J. Appl. Meteor.*, **32**, 1352-1364.

Budyko, M.I., 1974: *Climate and life*. Academic Press, 510 pp.

Bras, R.L., 1990: *Hydrology. An introduction to hydrologic science*. Addison-Wesley, 643 pp.

Brutsaert, W., 1982: *Evaporation into the atmosphere*. D. Reidel, 299 pp.

Camillo, P.J., R.J. Gurney, and T.J. Schmugge, 1983: A soil and atmospheric boundary layer model for evapotranspiration and soil moisture studies. *Water Resources Res.*, **19**, 371-380.

Chen, F., and R. Avissar, 1994: The impact of land-surface wetness heterogeneity on mesoscale heat fluxes. *J. Appl. Meteor.*, **33**, 1323-1340.

Choudhury, B.J., 1991: Multispectral satellite data in the context of land surface heat balance. *Rev. Geophys.*, **29**, 217-236.

Clapp, R.B., and G.M. Hornberger, 1978: Empirical equations for some soil hydraulical properties. *Water Resources Res.*, **14**, 601-604.

Claussen, M., 1991: Estimation of areally-averaged surface fluxes. *Bound. Lay. Meteor.*, **54**, 387-410.

Claussen, M., 1993: Flux aggregation at large scales: on the limits of validity of the concept of blending height. Max-Planck-Institut für Meteorologie Rep. No. 111, 16 pp, Hamburg, Germany.

Cogley, J.G., A.J. Pitman, and A. Henderson-Sellers, 1990: A land surface for large scale climate models. *Technical Note* **90-1**, Trent University, Peterborough, Ontario, K9J 7B8, Canada.

Cosby, B.J., G.M. Hornberger, R.B. Clapp, and T.R. Ginn, 1984: A statitistical exploration of the relationships of soil moisture characteristics to the physical properties of soils. *Water Resources Res.*, **20**, 682-690.

Cuenca, R.H., and J. Noilhan, 1991: Use of soil moisture measurements in hydrological balance studies. *Land surface evaporation: Measurement and parametrization*, T.J. Schmugge and J.C. André, Eds., Springer, 287-299.

de Vries, D.A., 1958: Simultaneous transfer of heat and moisture in porous media. *Trans. Am. Geophys. Union*, **39**, 909-916.

de Vries, D.A., 1963: Thermal properties of soils. *Physics of plant environment.* W.R. van Wijk, Ed., North Holland, 210-235.

de Vries, D.A., 1975: Heat transfer in soils. *Heat and mass transfer in the biosphere. Part1: Transfer processes in the plant environment.* D.A. de Vries and N.H. Afgan, Eds., Wiley, 4-28.

Daley, R., 1991: *Atmospheric data analysis*. Cambridge Univ. Press, Cambridge, 458 pp.

Deardorff, J.W., 1978: Efficient prediction of ground surface temperature and moisture, with inclusion of a layer of vegetation. *J. Geophys. Res.*, **83C**, 1889-1903.

Delworth, T.L., and Manabe, S. 1988: The influence of potential evaporation on the variabilities of simulated soil wetness and climate. *J. Climate*, **1**, 523-547.

© ECMWF, 2002

Delworth, T.L., and Manabe, S. 1989: The influence of soil wetness on near-surface atmospheric variability. *J. Climate*, **2**, 1447-1462.

Dickinson, R.E., 1984: Modeling evapotranspiration for three-dimensional climate models. *Climate processes and climate sensitivity. Geophys. Monogr.*, No. 29, Amer. Geophys. Union, 58-72.

Dickinson, R.E., 1988: The force-restore model for surface temperatures and its generalizations. *J. Climate*, **1**, 1086-1097.

Dickinson, R.E., 1992: Land surface. *Climate system modeling*, K.E. Trenberth, Ed., 149-171, Cambridge Univ. Press.

Dickinson, R.E., A. Henderson-Sellers, and P.J. Kennedy, 1993: Biosphere-atmosphere transfer scheme (BATS) Versaion 1e as coupled to the NCAR Community Climate Model. NCAR Technical Note, NCAR/TN-387+STR, 72pp.

Dickinson, R.E., A. Henderson-Sellers, P.J. Kennedy, and M.F. Wilson, 1986: Biosphere-atmosphere transfer scheme (BATS) for the NCAR community model. NCAR Technical Note, NCAR/TN-275+STR, 69pp.

Dickinson, R.E., A. Henderson-Sellers, C. Rosenzweig, and P.J. Sellers, 1991: Evapotranspiration models with canopy resistance for use in climate models, a review. *Agric. For. Meteorol.*, **54**, 373-388.

Dirmeyer, P.A., and J. Shukla, 1993: Observational and modeling studies of the influence of soil moisture anomalies on atmospheric circulation. *Prediction of interannual climate variations*, J. Shukla, Ed., Springer-Verlag, 1-23.

Dolman, A.J., S.J. Allen, and J. Lean, 1993: Climate simulations of the Sahel: a comparison with surface energy balance observations. *Exchange processes at the land surface for a range of space and time scales (Proc. Int. Symp., Yokohama, Japan, July1993)*, H. J. Bolle, Ed. *IAHS Publication* No. **212**. IAHS Press, Institute of Hydrology,Wallingford, Oxfordshire, UK, 513-519.

Dolman, A.J., and D. Gregory, 1992: Reply to comments by E.A. Eltahir and R.L. Bras on "The parametrization of rainfall interception in GCMs". *Quart. J. Roy. Meteor. Soc.*, **120**, 735.

Dooge, J., 1992a: Sensitivity of runoff to climate change: A Hortonian approach. *Bull. Amer. Meteor. Soc.*, **73**, 2013-2024.

Dooge, J., 1992b: Hydrologic models and climate change. *J. Geophys. Res.*, **97D**, 2677-1686.

Dorman, J.L., and P.J. Sellers, 1989: A global climatology for albedo, roughness length, and stomatal resistance for atmospheric general circulation models as represented by the Simple Biosphere Model (SiB). *J. Appl. Meteor.*, **28**, 833-855.

Douville, H., J.-F. Royer, and J.-F. Mahfouf, 1995: A new snow paramterization for the Météo-France climate model. Part I: Validation in stand alone experiments. Submitted to *Climate Dyn*.

Duchaufour, P., 1984: *Pédologie*. Masson, 220 pp.

Ducoudré, N.I., K. Laval, and A. Perrier, 1993: SECHIBA, a new set of parametrizations of the hydrological exchanges at the land-atmosphere interface within the LMD atmospheric general circulation model. *J. Climate*, **6**, 248-273.

Dümenil, L., and L. Bengtsson, 1993: Observational and modelling studies of the influence of land surface anomalies on atmospheric circulation (future directions). *Prediction of interannual climate variations*, J. Shukla, Ed., Springer-Verlag, 25-47.

Dümenil, L., and E. Todini, 1992: A rainfall-runoff scheme for use in the Hamburg climate model. *Advances in*

© ECMWF, 2002

theoretical hydrology. J.P.O'Kane, Ed.,Elsevier, 129-157.

Dunne, T., 1978: Field studies of hillslope flow processes. *Hillslope hydrology*, M.J. Kirkby, Ed., Wiley, 227-293.

Dyer, A.J., 1974: A review of flux-profile relations. *Bound.-Lay. Meteor.*, **1**, 363-372.

Eagleson, P.S., 1970: *Dynamic Hydrology*. Mc-Graw Hill, 462 pp.

Eagleson, P.S., 1978a: Climate, soil, and vegetation. 3. A simplified model of soil moisture movement in the liquid phase. *Water Resour. Res.*, **14**, 722-730.

Eagleson, P.S., 1978b: Climate, soil, and vegetation. 2. The distribution of annual precipitation derived from observed storm sequences. *Water Resour. Res.*, **14**, 713-721.

Eagleson, P.S., and Q. Wang, 1985: Moments of catchment storm area. *Water Resources Res.*, **21**, 1185-1194.

Eltahir, E.A.B., and R.L. Bras, 1993: Estimation of fractional coverage of rainfall in climate models. *J. Climate*, **6**, 639-644.

Emanuel, K.A., J.D. Neelin, and C.S. Bretherton, 1994: On large-scale circulations in convective atmospheres. *Quart. J. Roy. Meteor. Soc.*, **120**, 1111-1143.

Entekhabi, D. and P.S. Eagleson, 1989: Land surface hydrology parametrization for atmospheric general circulation models including subgrid scale spatial variability. *J. Climate*, **2**, 816-831.

Famiglietti, J.S. and E.F. Wood, 1994: Aggregation and scaling of spatially-variable hydrological processes, 3. A macroscale model of water and energy balance. *Water Resources Res.*

Federer, C.A., 1979: A soil-plant-atmosphere model for transpiration and availability of soil water. *Water Resour. Res.*, **15**, 555-562.

Fiedler, F., H.A. Panofsky, 1972: The geostrophic drag coefficient and the "effective" roughness length. *Quart. J. Roy. Meteor. Soc.*, **98**, 213-220.

Garratt, J.R., 1992: *The atmospheric boundary layer*. Cambridge Univ. Press, 318 pp.

Garratt, J.R., 1993: Sensitivity of climate simulations to land-surface and atmospheric boundary layer treatments - A review. *J. Climate*, **6**, 419-449.

Henderson-Sellers, A., Z.-L. Yang, and R.E. Dickinson, 1993: The project of intercomparison of land-surface parametrization schemes. *Bull. Amer. Meteor. Soc.*, **74**, 1335-1349.

Henning, D., 1989: *Atlas of the surface heat balance of the continents*. Gebrueder Borntraeger, 402 pp.

Hillel, D., 1982: *Introduction to soil physics*. Academic Press, 370 pp.

Högström, U., 1988: Non-dimensional wind and temperature profiles in the atmospheric surface layer: A re-evaluation. *Bound.-Lay. Meteor.*, **42**, 55-78.

Hollinger, S.E., and S.A. Isard, 1994: A soil moisture climatology of Illinois. *J. Climate*, **5**, 683-698. *J. Climate*, **7**, 822-833.

Horton, 1931: The field, scope and status of the science of hydrology. *Trans. Amer. Geophys. Union*, **12**, 189-202.

Jacobs, C.M.J, and H.A.R. de Bruin, 1992: The sensitivity of regional transpiration to land-surface characteristics: significance of feedback. *J. Climate*, **5**, 683-698.

Jacquemin, B., and J. Noilhan, 1990: Sensitivity study and validation of a land-surafce parametrization using the HAPEX-MOBILHY data set. *Bound.-Lay. Meteor.*, **52**, 93-134.

© ECMWF, 2002

Jaeger, L., 1983: Monthly and areal patterns of mean global precipitation. *Variations in the global water budget*. A. Street-Perrott, M. Beran, and R. Ratcliffe, Eds., D. Reidel, 129-140.

Jarvis, P.G., 1976: The interpretation of the variations in leaf-water potential and stomatal conductance found in canopies in the field. *Phil. Trans. Roy. Soc. London*, **B723**, 593-610.

Johnson, K.D., D. Entekhabi, and P.S.Eagleson, 1993: The implementation and validation of improved land-surface hydrology in an atmospheric general circulation model. *J. Climate*, **6**, 1009-1026.

Kaimal, J.J. and J.C. Finnigan, 1994: *Atmospheric boundary layer flows. Their structure and measurement*. Oxford Univ. Press, Oxford, 290 pp.

Kalnay, E., and M. Kanamitsu, 1988: Time schemes for strongly non-linear damping equations. *Mon. Wea. Rev.*, **116**, 1945-1958.

Kondo, J., N. Saigusa and T. Sato, 1990: A parametrization of evaporation from bare soil surfaces. *J. Appl. Meteor.*, **29**, 385-389.

Koster, R.D., and M.J. Suarez, 1992: Modeling the land surface boundary in climate models as a composite of independent stands. *J. Geophys. Res.*, **97D**, 2697-2715.

Kowalczyk, E.A., J.R. Garratt, and P.B. Krummell, 1991: A soil-canopy scheme for use in a numerical model of the atmosphere-1D stand-alone model. *CSIRO Division of Atmospheric Research Technical Paper* **23**, Commonwealth Scientific and Industrial Research, Mordialloc, Victoria, Australia, 56 pp.

Laval, K., 1988: Land surface processes. *Physically-based modelling and simulation of climate and climatic change - Part I*, M.E. Schlesinger, Ed., 285-306.

Legates, D.R., and C.J. Willmott, 1990: Mean seasonal and spatial variability in gauge-corrected, global precipitation. *Int. J. Climatol.*, **10**, 111-127.

Li, B., and R. Avissar, 1994: The impact of spatial variability of land-surface characteristics on land-surface heat fluxes. *J. Climate*, **7**, 527-537.

Liang, X., D. Lettenmaier, E.F. Wood, and S.J. Burges, 1994: A simple hydrologically based model of land surface water and energy fluxes for general circulation models. *J. Geophys. Res.*, **99D**, 14415-14428.

Mahfouf, J.F., 1991: Analysis of soil moisture from near-surface parameters: A feasibility study. *J. Appl. Meteor.*, **30**, 1534-1547.

Mahfouf, J.F., and B. Jacquemin, 1989: A study of rainfall interception using a land surface parametrization for mesoscale meteorological models. *J. Appl. Meteor.*, **28**, 1282-1302.

Mahfouf, J.F., A.O. Manzi, J. Noilhan, H. Giordani, M. Deque, 1993: The land surface scheme ISBA within the Meteo-France climate model ARPEGE. PartI: Implementation and preliminary results. *Note de Travail du Groupe de Meteorologie a Moyenne Echelle*, **30**, 43 pp.+fig. MeteoFrance, Toulouse, France.

Mahfouf, J.F., and J. Noilhan, 1991: Comparative study of various formulations from bare soil using in situ data. *J. Appl. Meteor.*, **30**, 1354-1365.

Mahfouf, J.-F., and J. Noilhan, 1994: Modélisation des échanges de surface dans les modèles météorologiques. *X Journées hydrologiques - ORSTOM* - Septembre 1994.

Mahrt, L., 1987: Grid-averaged surface fluxes. *Mon. Wea. Rev.*, **115**, 1550-1560.

Mahrt, L., and H.-L. Pan, 1984: A two-layer model of soil hydrology. *Bound.-Lay. Meteor.*, **29**, 1-20.

Manabe, S., 1969: Climate and the ocean circulation,1. The atmospheric circulation and the hydrologyof the earth's

© ECMWF, 2002

surface. *Mon. Wea. Rev.*, **97**, 739-774.

Marshall, T.J., and J.W. Holmes, 1988: *Soil physics*. Cambridge University Press, 374 pp.

Mascart, P., J. Noilhan, and H. Giordani, 1995: A modified parametrization of the surface layer flux-profile relationships using different roughness length values for heat and moisture. *Bound. Lay. Meteor*, in press.

Mason, P.J., 1988: The formation of aerially-averaged roughness lengths. *Quart. J. Roy. Meteor. Soc.*, **114**, 399-420.

Mason, P.J., 1992: Boundary-layer parametrization in heterogeneous terrain. *Proc. ECMWF Workshop on fine-scale modelling and the development of parametrization schemes, 16-18 September 1991*, ECMWF, Reading, UK, 275-288.

McCumber, M., and R.A. Pielke, 1981: Simulation of the effects of surface fluxes of heat and moisture in a mesoscale numerical model. 1. Soil layer. *J. Geophys. Res.*, **86C**, 9929-9938.

Miller, D.H., 1967: Sources of energy for thermodynamically-caused transport of intercepted snow from forest crowns. *Forest Hydrology*, W.E. Sopper and H.W. Lull (Eds.), 201-211. Pergamon, Oxford.

Miller, J.R., G.L. Russell, and G. Caliri, 1994: Continental-scale river flow in climate models. *J. Climate*, **7**, 914-928.

Miller, R.D., 1980: Freezing phenomena in soils. *Applications of soil physics*, D. Hillel, Ed., Academic Press, 254-299.

Milly, P.C.D., 1982: Moisture and heat transport of hysteretic, inhomogeneous porous media: A matric head-based formulation and a numerical model. *Water Resour. Res.*, **18**, 489-498.

Milly, P.C.D., 1991: A refinement of the combination equations for evaporation. *Surveys in Geophysics*, **12**, 145-154.

Milly, P.C.D., 1992: Potential evaporation and soil moisture in general circulation models. *J. Climate*, **5**, 209-226.

Milly, P.C.D., 1993: An analytical solution of the stochastic storage problem applicable to soil water. *Water Resour. Res.*, **29**, 3755-3758.

Milly, P.C.D., 1994: Climate, interseasonal storage of soil water, and the annual water balance. *Adv. Water Resour.*, **17**, 19-24.

Milly, P.C.D., and K.A. Dunne, 1994: Sensitivity of the global water cycle to the water-holding capacity of land. *J. Climate*, **7**, 506-526.

Mintz, Y., 1984: The sensitivity of numerically simulated climates to land-surface boundary conditions. *Global Climate*. J. Houghton, Ed., 79-105.

Mintz, Y., and Y.V.Serafini, 1992: A global monthly climatology of soil moisture and water balance. *Clim. Dynamics*, **8**, 13-27.

Monteith, J.L., 1965: Evaporation and environment. *19th Symp. Soc. Exp. Bio.*, 205-234.

Monteith, J.L., 1980: The development and extension of Penman's evaporation formula. *Applications of soil physics*, D. Hillel, Ed., Academic Press, 247-253.

Monteith, J.L., 1981: Evaporation and surface temperature. *Quart. J. Roy. Meteor. Soc.*, **107**, 1-27.

Namias, J., 1958: Persistence of mid-tropospheric circulations between adjacent months and seasons. *The atmosphere and sea in motion (Rossby memorial volume)*. B. Bolin, Ed., Rockfeller Institute Press, 240-248.

© ECMWF, 2002

Noilhan, J. and P. Lacarrère, 1995: GCM gridscale evaporation from mesoscale modeling. *J. Climate*, **8**, 206-223.

Noilhan, J., J. Mahfouf, A. Manzi, and S. Planton, 1993: Validation of land-surface parametrizations: Developments and experience at the French weather service. *Proc. Seminar ECMWF, 7-11 September 1992*, ECMWF, Reading, UK, 125-158.

Noilhan, J., and S. Planton, 1989: A simple parametrization of land surface processes for meteorological models. *Mon. Wea. Rev.*, **117**, 536-549.

Pan, H.-L., 1990: A simple parametrization scheme of evapotranspiration over land for the NMC medium-range forecast model. *Mon. Wea. Rev.*, **118**, 2500-1512.

Patterson, K.A., 1990: Global distribution of total and total-available soil water-holding capacities. Msc. Thesis, Univ. of Delaware, 119 pp.

Peixoto, J.P., and A. Oort, 1992: *Physics of climate*. American Institute of Physics, 520 pp.

Penman, H.L., 1948: Natural evaporation from open water, bare soil and grass. *Proc. Roy. Soc. London*, **A193**, 120-145.

Pitman, A.J., 1991: A simple parametrization of subgrid scale open water for climate models. *Clim. Dynamics*, **6**, 99-112.

Pitman, A.J., A. Henderson-Sellers, F. Abramopoulos, R. Avissar, G. Bonan, A. Boone, J.G. Cogley, R.E. Dickinson, M. Ek, D. Entekhabi, J. Famiglietti, J.R. Garratt, M. Frech, A. Hahmann, R. Koster, E. Kowalczyk, K. Laval, L. Lean, T.J. Lee, D. Lettenmaier, X. Liang, J-F. Mahfouf, L. Mahrt, C. Milly, K. Mitchell, N. de Noblet, J. Noilhan, H. Pan, R. Pielke, A. Robock, C. Rosenzweig, S.W. Running, A. Schlosser, R. Scott, M. Suarez, S. Thompson, D. Verseghy, P. Wetzel, E. Wood, Y. Xue, Z-L. Yang, L. Zhang, 1992: Results from the off-line control simulation phase of the Project for Intercomparison of Landsurface Parameterisation Schemes (PILPS). *IGPO Publ. Series*, **7**, 47 pp.

Pitman, A.J., A. Henderson-Sellers, and Z.-L. Yang, 1990: Sensitivity of regional climates to localized precipitation in global models. *Nature*, **346**, 734-737.

Pitman, A.J., Z.-L. Yang, J.G Cogley, and A. Henderson-Sellers, 1991: Description of bare essentials of surface transfer for the Bureau of Meteorology Research Centre AGCM. Bur. Meteor. Res. Rep. No.32, 86pp.

Pitman, A.J., Z.-L. Yang, and A. Henderson-Sellers, 1993: subgrid scale precipitation in AGCMs: re-assessing the land surface sensitivity using a single column model. *Clim. Dynamics*, **9**, 33-41.

Philip, J.R., 1957: Evaporation, and moisture and heat fields in the soil. *J. Meteor.*, **14**, 354-366.

Philip, J.R., and D.A. de Vries, 1957: Moisture movement in porous materials under temperature gradients. *Trans. Am. Geophys. Union*, **38**, 222-232.

Priestley, C.H.B., and R.J. Taylor, 1972: On the assessment of surface heat flux and evaporation using large-scale parameters. *Mon. Wea. Rev.*, **100**, 81-92.

Richards, L.A., 1931: Capillary conduction of liquids through porous mediums. *Physics*, **1**, 318-333.

Richardson, L.F., 1922: *Weather prediction by numerical process*. Cambridge Univ. Press, reprinted Dover, 1965, 236 pp.

Robock, A., K.Y. Vinnikov, C.A. Schlosser, N.A. Speranskaya, and Y. Xue, 1995: Use of midlatitude soil moisture and meteorological observations to validate soil moisture simulations with biosphere and bucket models. *J. Climate*, **8**, 15-35.

© ECMWF, 2002

Rowntree, P.R., 1991: Atmospheric parametrization schemes for evaporation over land: basic concepts and climate modeling aspects. *Land surface evaporation: Measurement and parametrization*, T.J. Schmugge and J.C. André, Eds., Springer, 5-29.

Russell, G.L., and J.R. Miller, 1990: Global river runoff calculated from a global atmospheric general circulation model. *J. Hydrol.*, **117**, 241-254.

Rutter, A.J., K.A. Kershaw, P.C. Robins, and A.J. Morton, 1972: A predictive model of rainfall interception in forests. I. Derivation of the model from observations in a plantation of Corsican pine. *Agric. Meteor.*, **9**, 367-384.

Rutter, A.J., A.J. Morton, and P.C. Robins, 1975: A predictive model of rainfall interception in forests. II. Generalization of the model and comparison with observations in some coniferous and hardwood stands. *J. Appl. Ecol.*, **12**, 367-380.

Sasamori, T., 1970: A numerical study of atmospheric and soil boundary layers. *J. Atmos. Sci.*, **27**, 1122-1137.

Sausen, R., S. Schubert, and L. Dümenil, 1994: A model of river runoff for use in coupled atmosphere-ocean models. *J. Hydrol.*, **155**, 337-352.

Schmugge, T.J., and F. Becker, 1991: Remote sensing observations for the monitoring of land-surface fluxes and water budgets. *Land surface evaporation: Measurement and parametrization*, T.J. Schmugge and J.C. André, Eds., Springer, 337-347.

Schulin, R., H. Flühler, H.M. Selim, B. Sevruk, and P.J. Wierenga, 1992: Soil moisture. Op. Hydrology Rep. No. 35, B. Sevruk, Ed., WMO No. 749, Part III, 219-283.

Segal, M., R. Avissar, M.C. McCumber, and R.A. Pielke, 1988: Evaluation of vegetation effects on the generation and modification of mesoscale circulations. *J. Atmos. Sci.*, **45**, 2268-2292.

Sellers, P.J., 1985: Canopy reflectance, photosynthesis and transpiration. *Int. J. Remote Sensing*, **6**,1335-1372.

Sellers, P.J., 1992: Biophysical models of land surface processes. *Climate system modeling*, K.E. Trenberth, Ed., 451-490, Cambridge Univ. Press.

Sellers, P.J., F.G. Hall, G. Asrar, D.E. Strebel, and R.E. Murphy, 1988: The First ISLSCP Field Experiment (FIFE). *Bull. Amer. Meteor. Soc.*, **69**, 22-27.

Sellers, P.J., F.G. Hall, G. Asrar, D.E. Strebel, and R.E. Murphy, 1992: An overview of the First International Satellite Land Surface Climatology Project (ISLSCP) Field Experiment (FIFE). *J. Geophys. Res.*, **D17**, 18345-18371.

Sellers, P.J., F.G. Hall, H. Margolis, B. Kelly, D. Baldocchi, J. denHartog, J. Cihlar, M. Ryan, B. Goodison, P. Crill, J. Ranson, D. Lettenmaier, and D. Wickland, 1995: The Boreal Ecosystem-Atmosphere Study (BOREAS): An overview and early results from the 1994 field year. Submitted to *Bull. Amer. Meteor. Soc.*

Sellers, P.J., and J.G. Lockwood, 1981: A computer simulation of the effects of differing crop types on the water balance of small catchments over long time periods. *Quart. J. Roy. Meteor. Soc.*, **107**, 395-414.

Sellers, P.J., Y. Mintz, Y.C. Sud, and A. Dalcher, 1986: A simple biosphere model (SiB) for use within general circulation models. *J. Atmos. Sci.*, **43**, 505-531.

Sellers, P.J., W.J. Shuttleworth, J.L. Dorman, A. Dalcher, and J.M. Roberts, 1989: Calibrating the simple biosphere model for Amazonian tropical forest using field and remote sensing data. Part I: Average calibration with field data. *J. Appl. Meteor.*, **28**, 727-759.

Shuttleworth, W.J., 1988a: Evaporation from Amazon rainforest. *Proc. R. Soc. Lond.*, **B233**, 321-346.

Shuttleworth, W.J., 1988b: Macrohydrology - The new challenge for process hydrology. *J. of Hydrol.*, **100**, 31-56.

© ECMWF, 2002

Shuttleworth, W.J., 1991: Insight from large-scales observational studies of land/atmosphere interactions. *Land surface-atmosphere interactions for climate modeling. Observation, models and analysis.* E.F. Wood, Ed.,Kluwer, 3-30.

Shuttleworth, W.J., 1993a: The soil-vegetation-atmosphere interface. *Energy and water cycles in the climate system*. E. Raschke and D. Jacob, Eds., NATO ASI Series vol. 15, Springer, 323-364.

Shuttleworth, W.J., 1993b: Evaporation. *Handbook of Hydrology*, D.R. Maidment, Ed., McGraw-Hill, 4.1-4.53.

Shuttleworth, W.J., J.H.C. Gash, C.R. Lloyd, C.J. Moore, J. Roberts, A.O. Marques-Filho, G. Fish, V.P. Silva-Filho, M.N.G. Ribeiro, L.C.B. Molion, L.D.A. Sá, J.C.A. Nobre, O.M.R. Cabral, S.R. Patel, and J.C. Moraes, 1984: Eddy correlation measurements of energy partition for Amazonian forest. *Quart. J. Roy. Meteor. Soc.*, **110**, 1143-1162.

Strauss , B., and A. Lanzinger, 1993: Overview of validation of direct model output. *Validation of models over Europe, ECMWF Seminar 7-11 Sept. 1992*, ECMWF, Shinfield Park, Reading RG2 9AX, UK, 93-104.

Stricker, J.N.M., C.P. Kim, R.A. Feddes, J.C. van Dam, P.Droogers, and G.H. de Rooij, 1993: The terrestrial hydrological cycle. *Energy and water cycles in the climate system*. E. Raschke and D. Jacob, Eds., NATO ASI Series vol. 15, Springer, 419-444.

Stull, R.B., 1988: *An introduction to boundary layer meteorology.* Kluwer, 666 pp.

Thomas, G., and A. Henderson-Sellers, 1991: An evaluation of proposed representations of subgrid hydrologic processes in climate models. *J. Climate*, **4**, 898-910.

Tiedtke, M., 1989: A comprehensive massflux scheme for cumulus parametrization in large-scale models. *Mon. Wea. Rev.*, **117**, 1777-1798.

UNESCO, 1974: *Discharge of selected rivers of the world*. UNESCO, Paris, 124 pp.

Verseghy, D.L., 1991: CLASS-A Canadian land surface scheme for GCMs. I. Soil model. *Int. J. Climatol.*, **11**, 111-133.

Verseghy, D.L., N.A. McFarlane, and M. Lazare, 1993: CLASS-A Canadian land surface scheme for GCMs, II. Vegetation model and coupled runs. *Int. J. Climatol.*, **13**, 347-370.

Verstraete, M.M., and R.E. Dickinson, 1986: Modeling surface processes in atmospheric general circulation models. *Ann. Geophys. Ser. B*, **4**, 357-364.

Vinnikov, K.Y., and I.B. Yeserkepova, 1991: Soil moisture empirical data and model results. *J. Climate*, **4**, 66-79.

Viterbo, P., and A.C.M. Beljaars, 1995: An improved land surface parametrization scheme in the ECMWF model and its validation. Accepted for publication in *J. Climate*.

Viterbo, P., and P. Courtier, 1995: The importance of soil water for medium-range weather forecasting. Implications for data assimilation. *International workshop of slowly varying components of predictable atmospheric motions*, Beijing, China, 7-10 March 1995. PWPR Rep. Ser. No. 6, WMO/TD No. 652, 121-130.

Viterbo, P. and L. Illari, 1994: The impact of changes in the runoff formulation of a general circulation model on surface and near-surface parameters. *J. Hydrol.*, **115**, 325-336.

Wallace, J.S., I.R. Wright, J.B. Stewart, and C.J. Holwill, 1991: The Sahelian Energy Balance Experiment (SEBEX): ground based measurements and their potential for spatial extrapolation using satellite data. *Advances in Space Res.*, **11**, 131-141.

Wallis, J.R., D. Lettenmaier, and E. Wood, 1991: A daily hydroclimatological data set for the conterminous US. *Water Resour. Res.*, **27**, 1657-1663.

© ECMWF, 2002

Walsh, J.E., W.H. Jasperson, and B. Ross, 1985: Influences of snow cover and soil moisture on monthly air temperature. *Mon. Wea. Rev.*, **113**, 756-768.

Wang, Q.J., 1992: Analytical and numerical modelling of unsaturated flow. *Advances in theoretical hydrology.* J.P.O'Kane, Ed.,Elsevier, 17-26.

Warrilow, D.L., and E. Buckley, 1989: The impact of land surface processes on the moisture budget ofa climate model. *Annales Geophysicae*, **7**, 439-450.

Warrilow, D.L., A.B. Sangster, and A. Slingo, 1986: Modelling of land-surface processes and their influence on European climate. UK Met. Office Rep., Met O 20, Tech. Note No. 38, 92 pp.

Wetzel, P.J., and J.T. Chang, 1987: Concerning the relationship between evapotranspiration and soil moisture. *J. Climate Appl. Meteor.*, **26**, 18-27.

Wetzel, P.J., and J.T. Chang, 1988: Evapotranspiration from nonuniform surfaces: A first approach for short-term numerical weather prediction. *Mon. Wea. Rev.*, **116**, 600-621.

Wieringa, J., 1986: Roughness-dependent geographical interpolation of surface wind speed averages. *Quart. J. Roy. Meteor. Soc.*, **112**, 867-889.

Williams, P.J., and M.W. Smith, 1992: *The frozen earth. Fundamentals of geocryology.* Cambridge Univ. Press, 308 pp.

Wood, E.F., D.P.Lettenmaier, and V.G. Zartarian, 1992: A land-surface hydrology parametrization with subgrid variability for general circulation models. *J. Geophys. Res.*, **97D**, 2717-2728.

Xue, Y., P.J. Sellers, J.L Kinter, and J. Shukla, 1991: A simplified biosphere model for global climate studies. *J. Climate*, **4**, 345-364.

© ECMWF, 2002